Causes for decadal trends in surface solar radiation in the Alpine region in the 1981-2020 period

Lucas Ferreira Correa[1], Doris Folini[1], Boriana Chtirkova[1] and Martin Wild[1]

[1]Institute for Atmospheric and Climate Sciences, ETH Zurich, Zurich, Switzerland.

Corresponding author: Lucas Ferreira Correa (lucas.ferreira@env.ethz.ch)

Key Points:

- Stations from the western and eastern Alps show different signs and transition periods in decadal trends of surface solar radiation.
- Low elevation stations show strong clear-sky trends, most likely associated with changes in aerosol emissions in Europe.
- Strong evidence suggests that changes in cloud optical depth and surface albedo can dominate SSR decadal trends at high elevation stations.

Abstract

Extending across seven countries, the Alps represent an important element for climate and atmospheric circulation in Central Europe. Its complex topography affects processes on different scales within the atmospheric system. This is of major relevance for the decadal trends in surface solar radiation (SSR), also known as global dimming and brightening (GDB). In this study we analysed data from 38 stations in and around the Swiss and Austrian Alps, over a period ranging from the 1980s up to the 2020s, with the aim of characterizing the spatio-temporal variations of the GDB and understanding the causes for such trends in this region. Our results show a different behavior in the SSR decadal trends in the western part of the Alps in comparison to the eastern part. Our results also suggest a remarkable difference between the causes of such trends at the stations at low altitudes in comparison to the stations at higher altitudes. Significant contribution from cloud optical depth and surface albedo to the SSR decadal trends at high elevation sites were found, in contrast to a strong clear-sky forcing that dominates at low elevations. Results from previous literature and available data suggest that cloud optical depth changes at high altitudes and clear-sky forcing at low altitudes could be associated with the indirect and direct aerosol effects, respectively, due to differing pollution levels at low and high elevation sites.

Plain Language Summary

The incidence of surface solar radiation (SSR) is not constant, nor spatially homogeneous over decades around the globe. It undergoes trends, also known as Global Dimming (negative) or Brightening (positive). Such trends can have different causes, such as changes in cloudiness and aerosol concentrations. In regions with complex topography, like the Alps, understanding the processes leading to such trends might be challenging. In this study we investigated the causes of decadal trends in SSR at 38 stations in the Alpine region. The results show distinctly different decadal trends in SSR between the stations in the western and those in the eastern part of the Alps. We also identified that altitude plays a major role for the causes of the trends. While at low elevations changes in aerosol concentrations seem to largely affect long-term SSR, at high altitude stations the changes in surface reflectivity and optical properties of clouds seem to dominate. This latter effect might be, however, also associated with changes in aerosol concentrations, since the amount of aerosols present in the cloud formation process significantly affects the cloud optical properties.

1 Introduction

The complexity of the Alpine region topography represents a challenge for many atmospheric and climate studies. In complex terrain, orographic forcing and local circulation features generate several phenomena which cover different scales of the atmospheric processes (Serafin et al., 2018). From a radiative perspective, this is especially important because it affects key processes affecting the energy balance, such as the aerosol transport (Rotach and Zardi, 2007) and cloud formation. Previous studies have investigated the energy budget in the alpine region (e.g. Ruckstuhl et al., 2007; Philipona, 2013), but the causes of decadal trends in

downward surface solar radiation (SSR) have not yet been deeply explored with focus on the Alpine region and its complex terrain.

Also known as Global Dimming and Brightening (Gilgen et al., 1998; Wild, 2005; Wild 2009), decadal trends in SSR have been an object of study for decades, due to their importance for various aspects of the climate system such as the hydrological cycle and energy budget. Pioneering studies in the late 1980s and early 1990s (e.g. Ohmura and Lang, 1989; Russak, 1990; Dutton et al., 1991; Stanhill and Moreshet, 1992) have for the first time presented evidence that the SSR was not constant over time, but exhibited decadal trends. Later publications (e.g. Wild 2009) have pointed out three main periods in the 20th century over Europe: a positive trend before the 50s also referred to as "early brightening"; a negative trend between the 1950s and the 1980s also referred to as "dimming"; and a follow-up period of positive trends also known as "brightening".

Regarding the causes of GDB, several studies (e.g. Power, 2003; Wild et al, 2005; Streets et al., 2009; Manara et al., 2016, Wild et al., 2021) have attributed the dimming and subsequent brightening in Europe to changes in aerosol loadings. Changes in emission regulations enforced from the 80s onwards in many European countries might have been a major cause for the decrease in AOD, which reduced the direct aerosol effect in most of Central and Southern Europe and resulted in an increase of SSR (brightening period). Other authors (Stjern et al., 2009) associated the GDB trends in northern Europe with changes in cloud cover. Even though Krüger and Graßl (2002) have identified a pronounced decrease in cloud albedo in Europe during the period of decreasing aerosols in the 1980s and 1990s, Ruckstuhl et al. (2010) did not find evidence of a significant indirect aerosol effect on SSR changes at 15 lowland stations (altitude lower than 1000 masl) in Switzerland during the same period. Folini et al. (2017) and Chtirkova et al. (2022) highlighted that the effect of internal variability at individual locations should not be neglected. All of these studies provide evidence for the existence of different players controlling the decadal SSR trends, from both natural and anthropogenic origins. Thus, a careful analysis is required to link SSR decadal trends to their causes.

In the present study, we analyze the spatio-temporal variations of the decadal trends in SSR in the alpine region and its underlying causes, contrasting the trends and causes in different parts of the Alps and at different altitudes. For this purpose we use data from 38 stations in and around the Swiss and Austrian Alps, at different altitudes. The time span depends on the data availability at each station, but ranges from the 1960s to the 2020s. The objective is to answer whether the GDB trends in the region are similar within the whole mountain range and to understand which processes control the trends in different areas and at different altitudes.

2 Data and Methods

2.1 Data

SSR daily means from 38 stations in the Swiss and Austrian Alpine region with data ranging from the 1960s until the 2020s were available for this study. Since the number of stations with available data decreases dramatically before 1981, the analyses were focused on the

1981-2020 period. The stations with radiation data used in this study are listed in Table 1 and shown in Figure 1. The data was collected from the World Radiation Data Center (WRDC - Voeikov Main Geophysical Observatory, 2022), from the Baseline Surface Radiation Network (BSRN - Ohmura et al., 1998; Driemel et al., 2018), from the repository of the Federal Office of Meteorology and Climatology of Switzerland (IDAWEB repository, Meteoswiss, 2023 - https://gate.meteoswiss.ch/idaweb) and from the GeoSphere Austria (GeoSphere Austria Data Hub, 2023 - https://data.hub.zamg.ac.at) which all provide data with at least daily resolution. Daily resolution is a prerequisite for the estimation of clear-sky trends as described in Correa et al. (2022). The altitudes of the stations range from 157 to 3580 meters above sea level.

In addition, synop cloud cover (in oktas) and sunshine duration (SD) were collected, when available, from the European Climate Assessment and Dataset (ECAD - Klein Tank et al., 2002), IDAWEB and GeoSphere Austria. All variables were provided as daily values. Daily sunshine duration is provided in hours, with one decimal. Daily cloud cover from Swiss stations is the average of 24 hourly observations per day, and from Austrian stations is the average of observations at 7, 14 and 19 CET. Individual synop cloud cover observations are given in integers from 0 to 8, and daily averages are rounded to the nearest integer, thus daily cloud cover acquired is an integer from 0 to 8. The cloud cover data is also used to calculate the Cloud Cover Radiative Effect (CCRE), following the procedure described by Norris and Wild (2007). The CCRE is an estimation of the change in SSR produced by changes in cloud cover.

For the assessment of aerosols, AOD data from the Copernicus Atmosphere Monitoring Service (CAMS) Reanalysis (Innes et al., 2019) for the period 2003-2020 was also analysed. For this dataset we obtained the monthly means, and the spatial resolution is of approximately 80 km. Further analysis of surface albedo and water vapour content were done using ERA5 reanalysis data (Hersbach et al., 2020). For the water vapour analysis we used total column water vapour, provided in units of kg/m^2, which considering a unit density of water, can be assumed the same unit as millimeters (mm). As this is the unit widely used for precipitation, we use mm. According to the available documentation on the ERA5 radiation quantities (Hogan, 2015), surface albedo should be calculated using Surface net Solar Radiation (SSR_{ERA5}) and Surface Solar Radiation Downwards ($SSRD_{ERA5}$), according to the formula: Surface Albedo = 1 - $SSR_{ERA5}/SSRD_{ERA5}$. We used this procedure to calculate the surface albedo used in this study. The ERA5 quantities used in this study had 0.25 degrees of horizontal resolution, monthly time resolution, and were available for the 1979-2020 period.

The directly measured variables (i.e. SSR and cloud cover) were converted from daily to monthly and further annual values by simple averaging the daily values and monthly values respectively. Monthly means are only calculated when at least 70% of the data in a month is available. Annual means are calculated only when 10 or more months are available, with any missing months being replaced by the climatology. After this averaging process the cloud cover data, which is originally given as integers from 0 to 8, results in values from 0 to 8 in intervals of 0.1.

Station	Altitude	Data availability	Clear-sky from Synop	True overcast	Source
Basel, Switzerland	316	1981-2022	Yes	Yes	IDAWEB
Geneva, Switzerland	420	1981-2022	Yes	Yes	IDAWEB
Payerne, Switzerland	491	1992-2021	Yes	Yes	BSRN
Zurich, Switzerland	436	1981-2022	Yes	Yes	IDAWEB
Cimetta, Switzerland	1661	1982-2022	No	No	IDAWEB
Davos, Switzerland	1590	1981-2022	No	No	IDAWEB
Evolene/Villa, Switzerland	1825	1986-2022	Yes	Yes	IDAWEB
Grimsel Hospiz, Switzerland	1980	1989-2022	Yes	Yes	IDAWEB
Col du Grand St-Bernard, Switzerland	2472	1982-2019	Yes	Yes	IDAWEB
Guetsch-Andermatt, Switzerland	2286	1981-2019	Yes	Yes	IDAWEB
Hinterrhein, Switzerland	1611	1981-2008	Yes	No	IDAWEB
Jungfraujoch, Switzerland	3580	1981-2022	Yes	Yes	IDAWEB
Le Moleson, Switzerland	1974	1982-2022	No	No	IDAWEB
Pilatus, Switzerland	2105	1981-2022	No	No	IDAWEB
Piz Corvatsch, Switzerland	3315	1981-2022	No	No	IDAWEB
Robiei, Switzerland	1898	1991-2022	No	No	IDAWEB
Saentis, Switzerland	2490	1981-2018	Yes	Yes	WRDC
Samedan, Switzerland	1708	1981-2022	Yes	Yes	IDAWEB
S. Bernardino, Switzerland	1638	1982-2022	Yes	Yes	IDAWEB
Weissfluhjoch, Switzerland	2691	1981-2019	Yes	Yes	IDAWEB

Zermatt, Switzerland	1638	1982-2022	Yes	Yes	IDAWEB
Graz, Austria	366	1964-2018	Yes	Yes	WRDC
Grossenzersdorf, Austria	157	1984-2018	Yes	Yes	WRDC
Innsbruck, Austria	579	1969-2018	Yes	Yes	WRDC
Salzburg, Austria	420	1964-2020	Yes	Yes	WRDC
Vienna, Austria	203	1964-2020	Yes	Yes	WRDC
Feuerkogel, Austria	1618	1964-2022	Yes	Yes	GeoSphere
Galzig, Austria	2079	1993-2022	Yes	Yes	GeoSphere
Hahnenkamm-Ehrenbachhoehe, Austria	1794	1993-2022	Yes	Yes	GeoSphere
Kolm Saigurn, Austria	1626	1996-2022	Yes	Yes	GeoSphere
Loferer Alm, Austria	1619	1995-2022	Yes	Yes	GeoSphere
Obertauern, Austria	1772	1995-2022	Yes	Yes	GeoSphere
Patscherkofel, Austria	2251	2008-2020	Yes	Yes	GeoSphere
Pitztaler Gletscher, Austria	2864	1994-2020	Yes	Yes	GeoSphere
Rudolfshuette, Austria	2317	1993-2020	Yes	Yes	GeoSphere
Schmittenhoehe, Austria	1956	1985-2022	Yes	Yes	GeoSphere
Sonnblick, Austria	3105	1964-2018	Yes	Yes	WRDC
Villacher Alpe, Austria	2140	2002-2022	Yes	Yes	GeoSphere

Table 1 - Radiation measurement stations used in the study. All-sky SSR and clear-sky SSR from Correa et al. (2022) available for all stations. Clear-sky from Synop or true overcast availability means the station was used in the referred composite. Availability of clear-sky Synop also implies the availability of Synop cloud cover data, used for cloud cover composites. Colors distinguish the stations for each one of the four categories considered for composites (Swiss low elevations, Swiss high elevations, Austrian low elevations, Austrian high elevations).

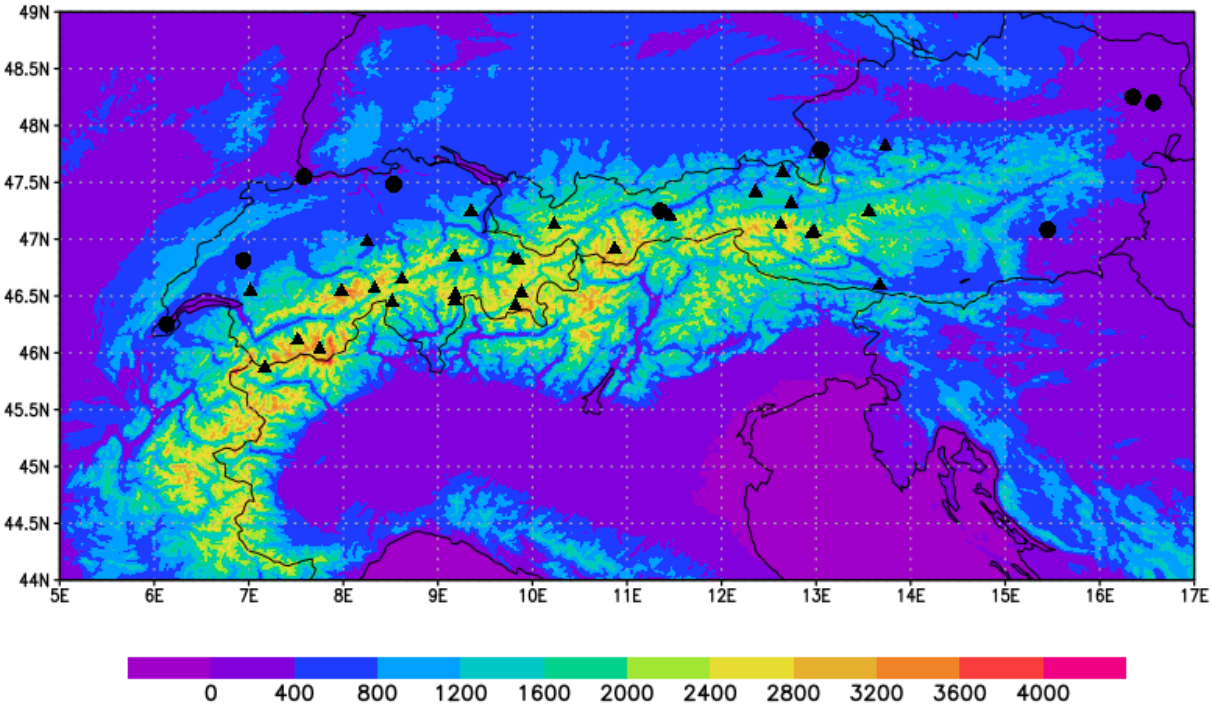

Figure 1 - Map of the altitudes (in meters) of the Alpine region and the locations of the stations used in this study. Triangles represent the high elevation stations (altitude >= 1500 meters) and circles represent the low elevation (altitude < 1500 meters) stations.

2.2 Derivation of clear-sky and true overcast time series

Clear-sky SSR time series were derived from the daily data based on 2 different methods: using (1) the method by Correa et al. (2022) and using (2) Synop cloud cover data (when available).

In (1), a site specific transmittance threshold is derived for each of the twelve calendar months of the year. To decide whether observed daily mean SSR reflects clear sky conditions, associated daily mean transmittance is compared to these thresholds. To obtain the transmittance thresholds, satellite cloud cover daily data is used as a proxy for clear-sky occurrence at each station. Then, by combining satellite cloud cover and transmittance data at the station (directly associating the station to its closest grid from the satellite data), optimal monthly transmittances thresholds are retrieved to remove days in which clouds significantly affected the transmittance, resulting in clear-sky time series. As the resulting clear-sky time series contains missing data on all days flagged as cloudy, special attention is required when converting daily data into monthly and annual values. Monthly values are only calculated when at least 2 days flagged as clear-sky

occur, otherwise the site specific climatology is used. The referred climatology is an annual cycle of monthly values calculated from the whole period of available (not missing) data. In the SSR time series used in this study this always meant the average obtained from more than 15 years of data (limited to the 1981-2006 period for the Swiss data due to homogeneity problem discussed in section 2.5). When calculating monthly means, the irradiance at the days flagged as clear-sky is normalised to the 15th day of the month, to avoid bias due to solar geometry. This is done by simply calculating the TOA daily irradiance at the 15th day of the referred month and the TOA daily irradiance at the day of the detected clear-sky. The ratio between the former and the latter is then multiplied by the daily clear-sky irradiance. Annual values are the mean of the 12 normalised monthly means, but are calculated only when at least 10 out of the 12 months had enough available data (i.e. no more than 2 months have the monthly value expressed as the climatology). The lack of more than 2 months is the reason for any missing annual values in the clear-sky from this method. This normalisation process when going from daily to monthly and then annual data is repeated in all further derivations used in this study (Synop clear-sky, overcast and true overcast time series). In the method (2), based on Synop cloud cover, we flagged any days with 2 or less oktas of cloud cover as clear-sky. As previously mentioned, cloud cover data is here referred to as the daily mean (i.e. only one value per day). The conversion from daily to monthly and annual clear-sky SSR values is done as described above.

Clear-sky time series allow the assessment of the cloud-free processes in the atmosphere, such as the SSR changes due to direct aerosol effect or the changes in water vapor content. In combination with all-sky SSR time series and cloud cover time series, it provides insight to the most important aspects regarding the SSR decadal variability. However, the context of this study also requires an assessment of the SSR variability due to cloud optical depth. The obvious choice to achieve this is to derive a SSR overcast time series using Synop cloud cover information, flagging all days with 8 oktas of cloud cover as overcast, as done in previous studies (e.g. Ruckstuhl et al., 2010). Nevertheless, these time series would still retain the SSR variability due to changes in cloud type. Ruckstuhl et al. (2010) have reported a positive trend in high clouds and a negative trend in cumulus clouds over Switzerland under overcast conditions in the period from 1981 to 2005. This “change” from low to high clouds would obviously exert a positive forcing on SSR, since high clouds are more transmissive to solar radiation. In order to minimize this effect in the SSR time series while keeping the effects of changes in cloud optical depth, we adapted the method by combining the Synop cloud fraction observations with sunshine duration observations. We used only days with 8 oktas of Synop cloud fraction and 0.0 hours of Sunshine duration to derive time series that from here on will be called “true overcast” SSR. As previously reported, these cloud fraction and sunshine duration values refer to the daily mean and daily total, respectively. Alternatively, this could have been done with information from low/high level clouds from Synop observations, which, however, was not available for this study. With these time series, we expect to avoid any days with non-overcast periods and days when the overcast condition is mostly due to high clouds, since, on such days, one could expect the heliograph to report non zero sunshine duration values. Comparisons between overcast and true overcast time series have shown irradiances up to 20% smaller in the latter, in addition to differences in the long term trends.

2.3 Data treatment and statistical methods

All SSR data here was preprocessed at the daily and monthly levels, to check for consistency and homogeneity, respectively. The physical and extremely rare limits established by Long and Dutton (2002) were considered. From personal communication with Meteoswiss (M. Begert, personal communication, June 29, 2023) we learned about the existence of major inhomogeneities in the Swiss irradiance data, due to changes in the instrumentation which occurred in the period 2006-2009 (precise date of the change being station dependent). Major efforts are currently under way at Meteoswiss to homogenise these data. However, at the time of this study, this is still an ongoing project and the homogeneized data have not yet been officially released by Meteoswiss. Nonetheless, after personal communication with Meteoswiss (M. Begert, personal communication, June 29, 2023) we were kindly granted access to a preliminary version of their homogenised dataset from 10 out of the 19 Meteoswiss stations, which we could use for comparison with the data available to us (but not for publication), in order to evaluate the consistency of our results with the homogenised unpublished dataset. A more detailed discussion of this comparison can be found in section 2.5.

Via personal communication with GeoSphere Austria personnel (V. Seitner, personal communication, July 5, 2023), we learned that, in contrast to the Swiss network, no major instrumentation changes occurred in the Austrian network. After all this information was collected, we still performed the Penalised Maximal F test proposed by Wang (2008) with the intent of identifying any additional non-documented inhomogeneities. Any correction due to doubtful data or inhomogeneity was done using nearby stations (not doubtful data from stations in a radius of 140 km) and the gap-filling procedure proposed by Begueria et al. (2019).

All the trends presented in this study were calculated from the annual anomalies time series using Linear Least Squares (LLS) when the residuals were normally distributed and using the Sen's Slope (Sen, 1968) and Mann-Kendall test (Mann, 1945; Kendall, 1975) when the residuals were not normally distributed (in the case of the cloud cover time series). Whether the residuals were normally distributed was tested using the Chi-squared test for variance in a normal population. The confidence intervals for the LLS trends were calculated using equation 4 from Nishizawa and Yoden (2005), taking into account any auto-correlation of the time series. The formula is directly applicable to annual data and gives the same confidence intervals as the commonly used methodology by Weatherhead et al. (1998).

2.4 Composite time series

To highlight the general aspects of the variability of SSR at low/high elevations and in Switzerland/Austria, we established composite time series. That is, we aggregated anomalies time series of the stations according to their elevation (high and low) and geographical location (Western - Switzerland; Eastern - Austria). These aggregated time series are expected to highlight the general behaviour of the stations within the same group, rather than local conditions of individual stations. We used 1500 meters of altitude as a threshold: stations above this altitude were classified as high elevation, and stations below this altitude as low elevation. Clear-sky composites were separated between the clear-sky time series derived using the method described in Correa et al. (2022) and the clear-sky time series derived using the Synop-based method,

meaning that each composite has two clear-sky time series. This was done to avoid potential inconsistencies due to the use of different clear-sky methods. True overcast composites included only the stations with both Synop cloud cover and sunshine duration data, resulting in less stations per composite. Information on which data was available for each station and which stations are used in each composite can be found on table 1.

2.5 Inhomogeneities in the Swiss radiation time series and time windows for trend analysis

The reported changes in the shortwave radiation measurement instruments in the Swiss network in the years 2006-2009 led to inhomogeneities in the SSR time series at the Swiss stations in this period. A comparison with the unreleased homogenised data from Meteoswiss (see Section 2.3) shows artificial jumps up to 10 W/m^2 (or around 7%) in SSR, and typical values around 7 W/m^2 (or around 5%). These inhomogeneities result in artificial SSR trends in the 1996-2020 period of up to 3.5 W/m^2 per decade. As mentioned earlier, the homogenised SSR data from the Swiss stations is at the time of this study not yet officially released, thus it cannot be directly used in this study, but only serve as a reference dataset. For these reasons, trends analyses for the Swiss stations do not consider a continuous time window including the 2006-2009 period. Rather, the Swiss trend analysis is performed for three main periods: 1981-1994, 1994-2006 and 2009-2020, thereby omitting the inhomogeneity issues between 2006 and 2009. As the date of change is station dependent, the years 2006 and 2009 could be included in the trend analyses. All-sky SSR trends for these three periods are identical to the homogenised reference dataset. For comparison, trends at the Austrian stations are calculated for the same three periods, but an additional time window covering the 1996-2020 period is also included. Plots of time series of SSR anomalies for the Swiss composites do not include the years 2007 and 2008. The time series before and after this period should be analysed independently. This issue did not affect the BSRN station Payerne. Thus, the trend for the entire available record covering the 1996-2020 period could be calculated for this station.

3 Results

We first present observational time series of all-sky and clear-sky SSR in Sections 3.1 and 3.2. Next, we examine in Section 3.3.1 cloud cover data and discuss its potential to explain the SSR observations presented, highlighting that cloud cover changes on their own cannot explain all aspects of observed all-sky SSR changes at most sites. Consequently, we turn to aerosol variability and cloud optical depth in Sections 3.3.2 to 3.3.3, using SSR under true overcast conditions as a proxy for the latter. Finally, in Section 3.4 we discuss the potential role of surface albedo and water vapour in the observed SSR trends.

3.1 Spatio-temporal differences of SSR decadal variability in the alpine region

Figure 2 shows the time series of all-sky SSR annual anomalies for the 4 composites analysed in this study (Swiss/Austrian high/low elevation stations). Swiss anomalies before 2007 were adjusted by +7 W/m^2, which was identified as a typical value for the artificial jump discussed in section 2.5. This adjustment was done purely for visual purposes, to better fit the

whole time series in one plot, and do not affect any trend calculations. This procedure was done only in the all-sky SSR plot.

Table 2 shows the trends for all-sky, clear-sky, true overcast SSR and for cloud fraction, as well as estimated CCRE in the time windows considered. The composites show the occurrence of a brightening in Austria already in the 1980s, highlighted by positive SSR trends in the 1981-1994 time window (6.6 ± 6.3 and 4.5 ± 9.7 W/m^2 per decade at low and high elevations, respectively). Statistically insignificant (at the 0.05 level) negative trends were observed in Switzerland in this period (-1.6 ± 7.0 and -2.4 ± 5.0 W/m^2 per decade at low and high elevations, respectively). In the 1990s, however, a brightening starts to be observed in Switzerland, indicated by statistically significant positive SSR trends in the 1994-2006 period. In Austria the trends were still positive, but they lost magnitude and/or statistical significance, suggesting a slow down in the brightening. This is confirmed by the Austrian trends in the 1996-2020 time window, which show a near zero trend at low elevations (0.4 ± 3.2 W/m^2 per decade), while a statistically significant dimming is observed at high elevations (-2.8 ± 2.7 W/m^2 per decade). The Swiss composites were not available for this period due to the homogeneity issues discussed in session 2.5. However, these issues do not apply to the low elevation Swiss station in Payerne, which shows a positive trend of 7.0 ± 2.8 W/m^2 per decade, in contrast to the dimming observed in the Austrian composites. In addition, the positive trends in the Swiss composites in the 2009-2020 period (statistically significant at low elevations and insignificant at high elevations) reinforce the occurrence of a persistent brightening in Switzerland in the first decades of the 21st century.

This reveals a significant contrast in the SSR trends between the western Alpine region, in Switzerland, and the eastern Alpine region, in Austria. The brightening starts earlier in Austria, but ends at the beginning of the 20th century, while in Switzerland the brightening starts later, but is maintained after the turn of the century. The contrast between low and high elevations is more closely examined in the following sections.

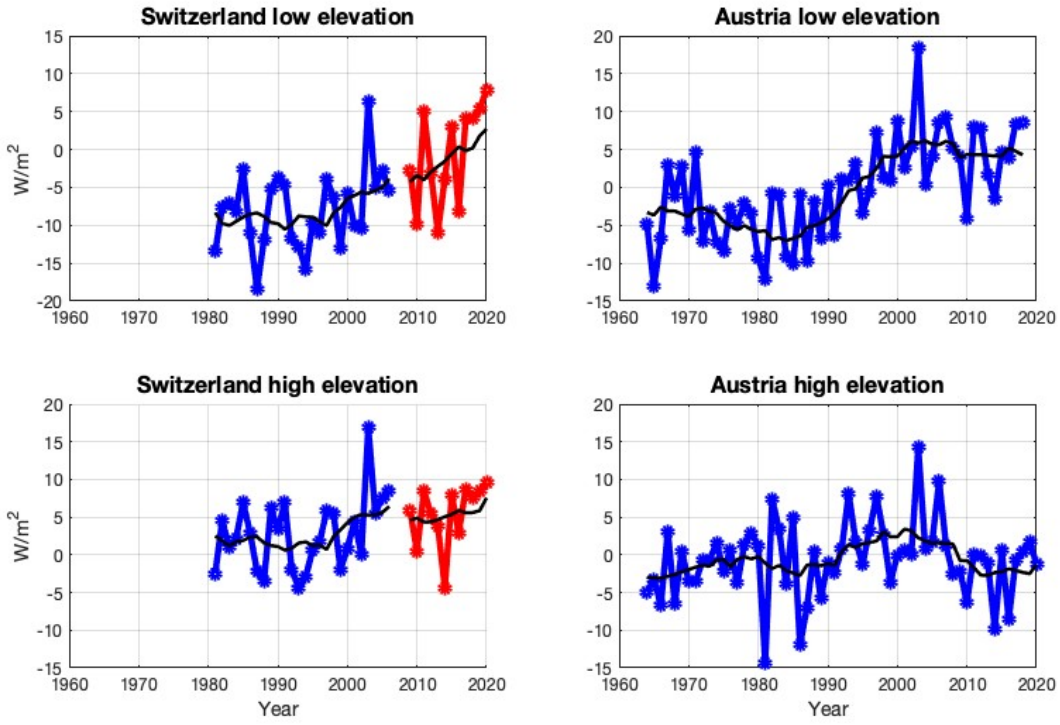

Figure 2 - Annual all-sky SSR anomalies time series for the 4 composites analyzed in this study. Swiss composites with two colors to denote the period before the inhomogeneity in the years 2007/2008 (blue) and after the inhomogeneity (red), thus both periods should be analysed independently. Anomalies before 2007 for the Swiss composites were artificially enhanced by 7 W/m² (to correct for the artificial jump around 2007/2008). This addition is purely for visual purposes, and did not affect the calculation of trends (shown in table 2) in any way. The black line represents the 11-year moving means; length of moving means shrinks at the border of the intervals to cover all existing elements. Y-axis might have different limits, but have the same range.

Composite	Time series	Period			
		1981-1994	1994-2006	2009-2020	1996-2020
Swiss low elevation	All-sky	-1.6 (± 7.0)	**8.1** (± 7.9)	**10.5** (± 10.3)	-
	Clear-sky Correa et al. (2022)	-1.5 (± 1.7)	**1.7** (1.7 ±)	**5.1** (2.5 ±)	-
	Clear-sky SYNOP	-1.4 (± 3.3)	**2.9** (± 1.8)	**6.8** (± 2.8)	-
	True Overcast	-0.8 (± 2.3)	-0.1 (± 2.3)	-1.6 (± 2.9)	-
	Cloud Cover	1.8 (-1.6; 4.6)	**-2.6** (-5.1; -0.1)	-5.9 (-10.5; 1.3)	-0.6 (-1.5; 0.6)
	CCRE	-1.7	2.4	5.5	0.5

Swiss high elevation	All-sky	-2.4 (± 5.0)	**8.1** (± 7.2)	4.7 (± 7.4)	-
	Clear-sky Correa et al. (2022)	0.2 (± 2.4)	**2.8** (± 1.3)	1.2 (± 4.4)	-
	Clear-sky SYNOP	-0.1 (± 2.5)	**2.8** (1.6 ±)	-0.9 (± 3.0)	-
	True Overcast	**-2.2** (± 2.1)	2.1 (± 3.3)	-	-
	Cloud Cover	0.0 (-2.6; 2.7)	-2.2 (-4.1; 1.2)	-3.4 (-9.4; 6.7)	0.2 (-0.8; 1.3)
	CCRE	0	2.2	3.4	-0.2
Austrian low elevation	All-sky	**6.6** (± 6.3)	6.4 (± 8.4)	5.7 (± 10.7)	0.4 (± 3.2)
	Clear-sky Correa et al. (2022)	3.0 (± 3.5)	**2.6** (± 1.6)	-1.7 (± 7.4)	0.0 (± 1.7)
	Clear-sky SYNOP	**9.8** (± 5.0)	**5.1** (± 3.1)	0.5 (± 4.6)	0.0 (± 1.7)
	True Overcast	-2.7 (± 4.5)	0.9 (± 2.2)	-2.7 (± 5.7)	-0.8 (± 1.1)
	Cloud Cover	-0.8 (-2.3; 1.4)	-1.6 (-3.4; 0.6)	-3.0 (-8.1; 4.1)	-0.2 (-1.1; 0.6)
	CCRE	0.9	1.8	3.4	0.2
Austrian high elevation	All-sky	4.5 (± 9.7)	3.9 (± 7.9)	2.4 (± 7.2)	**-2.8** (± 2.7)
	Clear-sky Correa et al. (2022)	-	2.0 (± 4.1)	0.0 (± 3.5)	**-3.9** (± 1.5)
	Clear-sky SYNOP	9.5 (± 14.4)	**4.0** (± 3.3)	-2.1 (± 4.6)	**-4.0** (± 1.8)
	True Overcast	-0.1 (± 12.3)	**8.5** (± 7.2)	**-5.2** (± 4.7)	**-3.8** (± 2.7)
	Cloud Cover	-0.3 (-2.0; 1.8)	**-1.9** (-4.4; 0.0)	-3.1 (-12.4; 8.5)	-0.2 (-1.6; 1.0)
	CCRE	0.3	2.2	3.7	0.2

Table 2 - Trends for all-sky, clear-sky (for both methods used) and true overcast SSR (in W/m^2 per decade), and cloud cover (in % per decade) during the 1981-1994, 1994-2006, 2009-2020 and 1996-2020 periods for the four composites analysed in this study. Uncertainties are in parenthesis. The last line of each composite includes the estimated CCRE (in W/m^2 per decade) based on the cloud cover trend for the period (not considering uncertainties). SSR trends calculated from annual values using Linear Least Squares and uncertainties (95% confidence level) calculated using eq. 4 from Nishizawa and Yoden (2005). Cloud cover trends calculated using Mann-Kendall test. Statistically significant trends (95% confidence level) are in bold. Swiss composites do not include trends for the 1996-2020 period due

to the inhomogeneity issue discussed in section 2.5. Any other missing trends denote not enough data for the composite in the period.

3.2 Clear-sky SSR

Figure 3 shows the time series of clear-sky SSR annual anomalies for the 4 composites analysed in this study, and for the two clear-sky derivation methods outlined in section 2. These time series are expected to show the variability when clouds do not play a role. Under these conditions, most periods of the composites keep the general behavior of the all-sky SSR. The Austrian composites show clear-sky brightening in the first two time windows, with a slow down at the turn of the century, resulting in a near zero trend at low elevations and statistically significant dimming at high elevations for the 1996-2020 period. It is important to point out the high year-to-year variability in the Austrian composites, especially in the clear-sky Synop composite. The Austrian low elevation clear-sky Synop composite was highly affected by the strong magnitude of negative anomalies in the Vienna station in the 1980s. The Austrian high elevation clear-sky Synop composite had only available data from two stations (Feuerkogel and Sonnblick) in the 1980s, which might explain the strong inter annual variability in that period. The Swiss composites show dimming and brightening in the first and second time windows respectively, both at low and high elevations, but distinct trends in the 2009-2020 period, with strong positive clear-sky SSR trends at low elevations and near zero trends at high elevations.

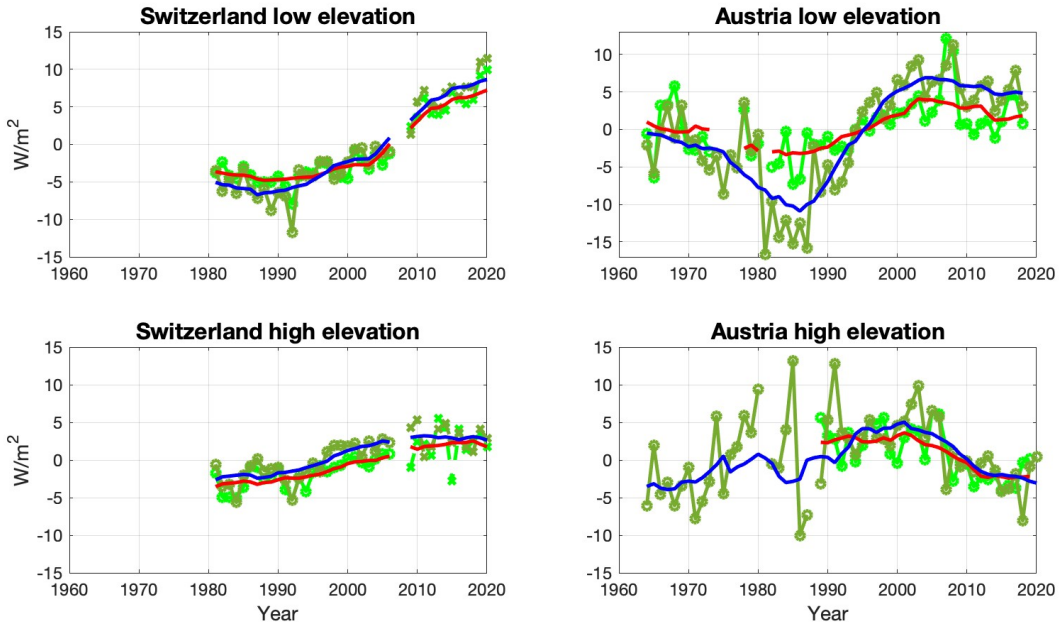

Figure 3 - Annual clear-sky SSR anomalies time series for the two clear-sky methods and four composites analyzed in this study. Time series in light green were derived with the method by Correa et al., (2022), time series in olive green were derived with SYNOP cloud cover data. Discontinuity followed by dashed lines in the Swiss composites denote the periods before and after the artificial jump discussed in section 2.5. Thus both parts should be interpreted independently. The solid red line represents the 11-year moving means of the green time series; the blue line represents the 11-year moving means of the of the orange time series. The Y-axis might have different limits, but have the same range.

Clear-sky SSR trends almost always agree in sign with the all-sky SSR trends at low elevations, showing statistical significance in almost all the cases where statistical significance is also found in all-sky (see table 2**)**. The only exception is the 2009-2020 period for Austrian low elevation composites for one of the two clear-sky methods. This agreement between all-sky and clear-sky at low elevations is a remarkable characteristic especially in the brightening period both in Switzerland and in Austria. This suggests that cloud-free processes have a major contribution to the observed all-sky SSR trends at low elevations. This is in line with previous studies which associated the changes in SSR decadal trends in Europe mostly to changes in aerosol loadings, which prevail in low level boundary layers (e.g. Wild et al, 2005; Streets et al., 2009; Manara et al., 2016, Wild et al., 2021).

At high elevations, on the other hand, a more complex situation is observed. The magnitude of the clear-sky SSR trends is in most cases smaller than at low elevations, and they do not always have the same sign as the all-sky SSR trends. The 2009-2020 period in Switzerland is a good example of that: while all-sky SSR at high elevations shows a statistically insignificant positive trend of 4.7 ± 7.4 W/m^2 per decade, the clear-sky SSR shows trends around zero (-0.9 ± 3.0 and 1.2 ± 4.4 for the two methods). The Austrian high elevation composite in the 1996-2020 period also shows a remarkable behaviour. But in that case, the observed clear-sky SSR dimming was stronger than the observed all-sky SSR dimming (both statistically significant). The overall situation at high elevation suggests that the non-cloud related processes can have significant contributions to the all-sky SSR trends (as the results indicate to be the case for the 1996-2020 period in Austria), but in most cases they are not enough to explain the observed all-sky SSR trends. Further analyses on the cloud and aerosol effects were done in order to gain a better understanding of the causes for such trends, and consequently the reasons for the differences between low and high elevations and between the western and eastern Alps.

3.3 The role of clouds and aerosols in the decadal SSR trends

The comparison between all-sky and clear-sky SSR changes in the different periods discussed in the previous section revealed, in general, important similarities at low elevations, while such similarities, despite also occurring for specific periods/composites/clear-sky methods, were not the norm at high elevations. This implies that clouds should be playing an important role in the all-sky SSR trends at the high altitude sites. At low elevations, the similarities between all-sky and clear-sky time series imply that the cloud-free processes dominate over the cloud effects.

3.3.1 Changes in cloud cover in the western and eastern Alps

The logical first step to initially verify the role of clouds in the Alpine region is through an analysis of the changes in cloud cover, which we pursued using composites of cloud cover from Synop observations. In figure 4 we display the annual mean cloud cover composites at the Austrian/Swiss Alps at low/high elevations.

No major long-term cloud cover trend was identified in the composites. Most periods showed slightly negative cloud cover trends in all composites. But only in the 1994-2006 period the trends were statistical significant, and only for the Swiss low elevation and Austrian high

elevation composites. The strongest trend in the period was at low elevations in Switzerland, with a -2.6 (-5.1; -0.1) % per decade. The only positive cloud cover trends are found at low elevations in the 1981-1994 period in Switzerland, but the trend was not statistically significant. This was the period with the biggest differences in the SSR trends between Austria and Switzerland. In the other periods the cloud cover trends were comparable between the two countries both at high and at low elevations. This is an interesting result in the context of the contrast between Swiss and Austrian SSR trends. Changes in cloud cover might have contributed to the difference in the SSR trends in the 1981-1994 period, but most likely did not play a role in the differences in the long-term SSR variability between western and eastern Alps thereafter. Another remarkable result is found for the Austrian high elevation composites in the period 1996-2020. That is a period of statistically significant negative SSR trends, but cloud cover trend is near zero (-0.2 [-1.6; 1.0] % per decade), indicating that changes in cloud cover are not a major cause for the dimming observed at high elevations in Austria at the beginning of the 21st century.

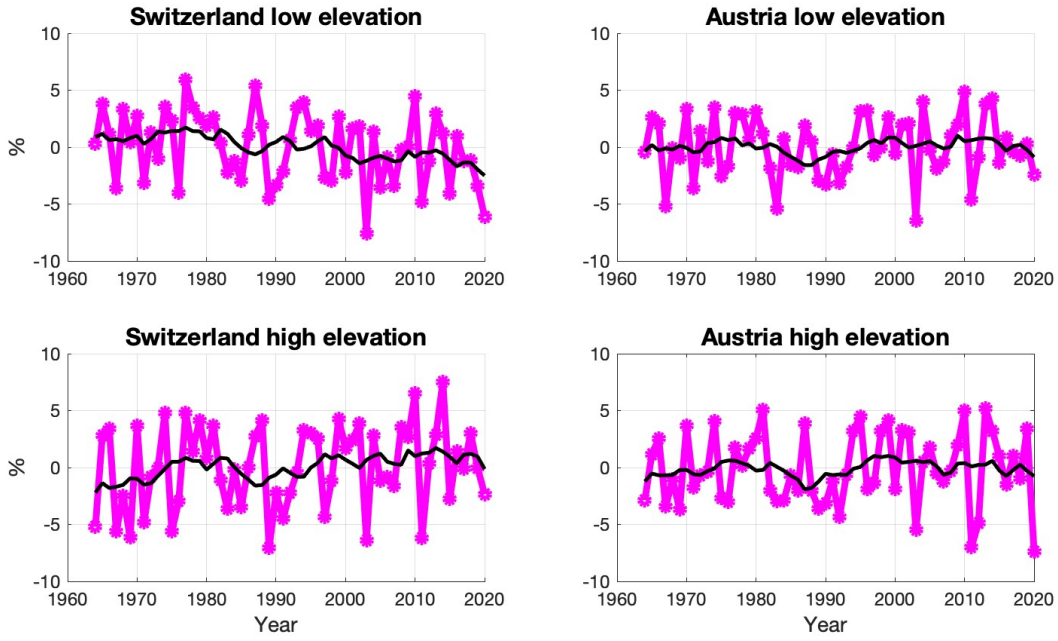

Figure 4 - Cloud cover annual anomalies time series from SYNOP observations for the four composites used in this study. The black line shows the 11-year moving means of the time series.

The overall scenario after analysis of the all-sky and clear-sky SSR and the cloud cover records, indicates that changes in cloud cover in most cases did not play a major role in the SSR decadal trends. That is especially the case at low elevations, where clear-sky SSR trends are consistent with the observed all-sky trends and the cloud cover trends are either near zero or have no statistical significance. The 1994-2006 period is the only period with statistically significant negative trends in cloud cover, thus the only period with significant contribution of changes in cloud cover to the SSR trends at low elevations. At high elevations the high uncertainties and/or low magnitudes of the cloud cover trends indicate that changes in cloudiness were not a factor of major relevance for the long term variability of SSR.

3.3.2 Aerosols and Cloud Optical Properties

The lack of an obvious cloud cover contribution to the SSR trends at high elevations turns our attention to the other potential causes for SSR decadal trends. Aerosols, for example, are another relevant factor for SSR long-term variability, thus the analysis of aerosol trends can add valuable information on the causes of the SSR trends. However, as indicated by the results from the clear-sky SSR time series, cloud-free processes might have contributed to the SSR trends at high elevations, but they are not enough to explain the whole trends. Changes in cloud optical properties are another potentially relevant contributor to SSR trends, and they can be associated with changes in aerosol loadings. Wild (2009) has introduced a conceptual framework on the role of aerosol and clouds in the dimming/brightening processes. The author argues that at pristine locations small changes in cloud condensation nuclei (CCN) potentially have an effective impact on cloud characteristics, thus a small increase in CCNs could result in an amplified reduction in SSR via aerosol indirect effect and vice versa. On the other hand, in highly polluted areas, cloud microphysics effects saturate, and an increase in aerosols may suppress cloud formation, resulting in an opposite effect on SSR trends compared to pristine regions (Wild 2009, 2012). Yang et al. (2021) have demonstrated this effect in China, which can be classified mostly as a highly polluted area. The high elevation Alpine stations analyzed in the present study have elevation above 1500 meters, being located above the lower layers of the atmosphere, where the major sources of aerosols are found and where the aerosol concentrations are usually higher. Thus, in the referred conceptual framework, these stations could be classified as pristine. This means that AOD trends can add information for the interpretation of both the direct aerosol effect and of the potential indirect aerosol effect.

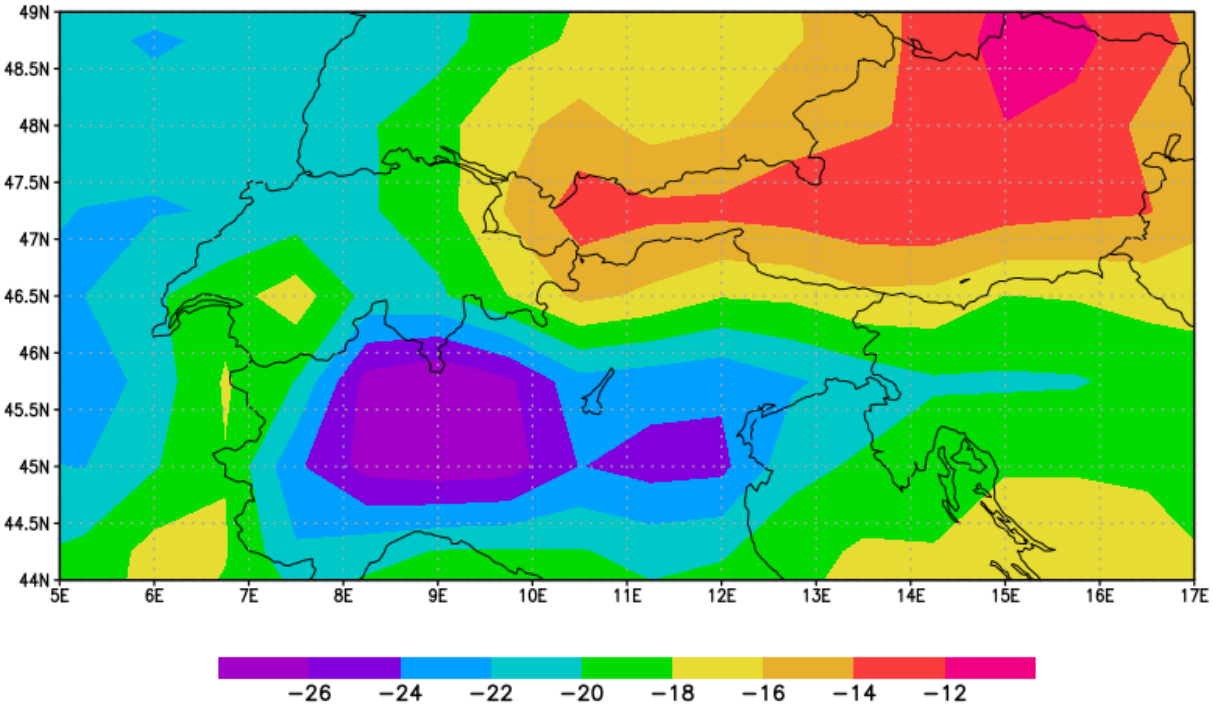

Figure 5 - AOD decadal trend (in % per decade) for the 2004-2019 period from the CAMS reanalysis.

Figure 5 shows the AOD for the 2004-2019 period from the CAMS reanalysis. The AOD trends show a remarkable contrast between the two countries. While the AOD reduction in almost the entire of Switzerland exceeds 20% per decade, in Austria the negative trend in AOD is not stronger than 15% per decade. This could be one relevant aspect of the difference between the observed SSR trends in Switzerland and in Austria. At low elevations the stronger reduction in AOD in Switzerland compared to Austria has potentially significantly contributed to a continued brightening in the first two decades of the 21st century in Switzerland, while in the Austria the weaker AOD reduction might have not been enough to maintain a positive trend in SSR.

Even though the same interpretation of the west-east contrast at low elevations can be applied to the high elevations, the lower concentration of aerosols at high altitudes leads to weaker direct aerosol effects. A direct consequence is a smaller magnitude of aerosol-forced clear-sky changes at high elevations. However, if the hypothesis of enhanced indirect aerosol effect due to pristine conditions at high elevations in the Alps is true, then as the direct aerosol effects weaken, the indirect aerosol effects should strengthen, and both should have the same trend sign. That is, reducing aerosols should lead to less attenuation of SSR by aerosols (direct

aerosol effect) but also should induce a reduction in cloud optical depth (indirect aerosol effect), both processes that exerting a positive forcing on SSR. Based on the physical processes discussed and on what we expect when assessing each time series, direct and indirect aerosol effect signs should dominate the clear-sky and true overcast SSR trends respectively. And, based solely on the aerosol effects, the trends should have the same signs in both time series.

On the top of a well documented reduction in aerosol loadings at the end of the 20th century in Europe, all the data presented here indicate a continued reduction in tropospheric aerosols in the whole of the Alpine region after 2000. The results show a stronger reduction in the western part of the Alps (Switzerland) than in the eastern part of the Alps (Austria). According to the referred conceptual framework (Wild 2009, 2012), such a decrease in aerosol concentrations in pristine regions as found at the high altitude Alpine stations could result in less bright clouds with shorter lifetimes, allowing for more solar radiation to reach the surface. Consequently, positive trends in true overcast at SSR at the turn of the century should be expected according to the conceptual framework, with higher magnitudes at high elevations. If this expectation holds, will be discussed in the next section.

3.3.3 True overcast SSR changes as a proxy for cloud optical depth changes

Aerosol measurements require a highly specialized instrumentation, and, for that reason, not all stations have such measurements. And even though the data presented in the previous section indicates a reduction in AOD, it does not contain any direct measurement of its impact on the cloud-aerosol interactions. Thus, in order to assess the effects of changes in cloud optical depth on SSR we used the time series of true overcast SSR (introduced in section 2) as a proxy. Figure 6 shows the true overcast time series for the four composites analysed in this study.

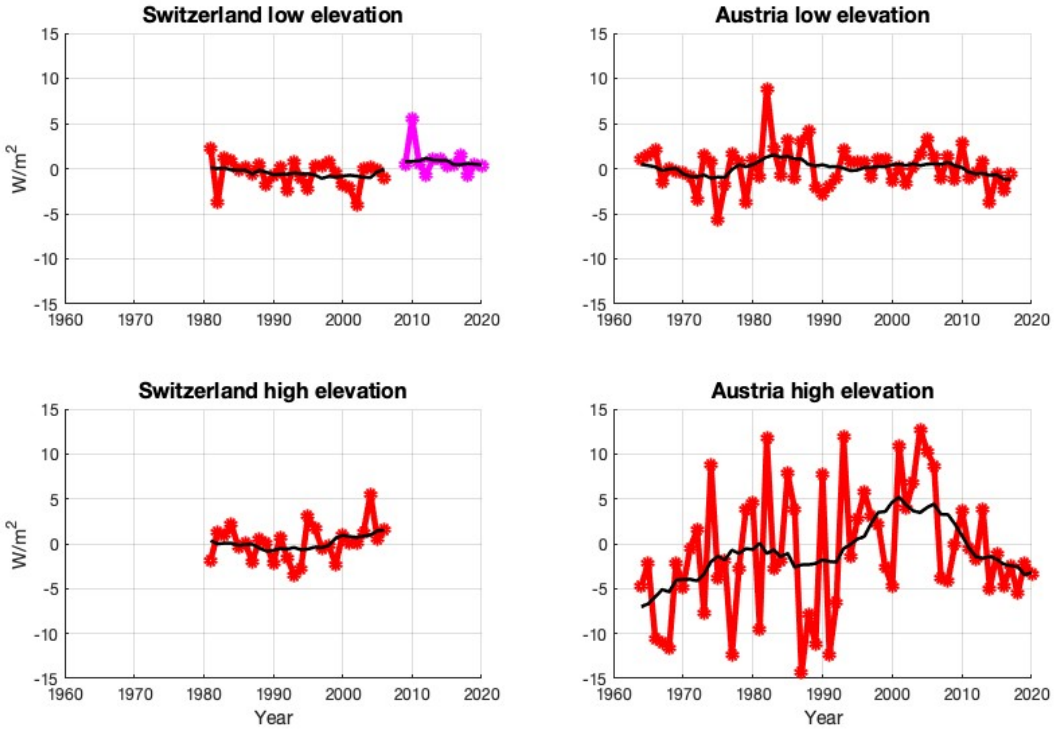

Figure 6 - True overcast SSR annual time series of the four composites analysed in this study. Black lines show the 11-year moving means. The part in magenta for the Swiss low elevation composites highlights the period after the change in instrumentation in the Swiss network. Thus, the red and magenta part should be analysed independently.

The expected positive trends in true overcast SSR at the turn of the 20th to the 21st century can be noted at the high elevation composited, as shown in Fig. 7. The strongest true overcast SSR trends are found in the 1994-2006 period, when the trend at high elevations in Austria is 8.5 ± 7.2 W/m² per decade. However, the 1996-2020 period at high elevations in Austria shows a negative true overcast SSR trend of -3.8 ± 2.7 W/m² per decade, opposite to what would be expected based on the AOD trends shown in figure 5. Nevertheless, this true overcast SSR trend is still in line with a negative clear-sky SSR trend observed in the same period. Another expected result observed in the true overcast SSR time series is the occurrence of stronger trends at high elevations. At low elevations the true overcast SSR trends are statistically insignificant for all the periods considered. For these composites the magnitude of the clear-sky SSR trends is significantly higher than true overcast SSR trends. At high elevations the true overcast trends are statistically significant and of larger magnitude than the clear-sky trends in most of the periods (see table 2).

The results suggest a stronger effect of indirect aerosol effects on SSR trends at the fairly pristine high elevations in comparison to the more polluted low elevations, in line with the conceptual framework by Wild (2009, 2012). While changes in cloud optical properties are negligible at low elevations (in line with Ruckstuhl et al., 2010), at high elevations they can make a significant contribution to the decadal SSR trends. When compared to the results

presented in the previous sections, true overcast SSR, and consequently cloud optical properties, seem to have contributed significantly to the observed SSR trends at high elevations in the 1981-1994 and 1994-2006 periods in Switzerland and in the 1994-2006 and 1996-2020 periods in Austria. Based on the results shown in the previous sections and on previous studies, the available evidence supports the existence of a potential link between the positive true overcast SSR trends in the 1994-2006 period with a decrease in aerosol loadings in the whole Alpine region. The negative true overcast SSR trend at the Swiss high elevations in the 1981-1994 period occurs in parallel to a negative clear-sky SSR trend at low elevations. This is in line with the expectation based on the physical interpretation of the impacts of the direct and indirect aerosol effects, and supports the hypothesis of relevant indirect aerosol aerosol effects at Swiss high elevations in this period. The negative trends in clear-sky and true overcast SSR could also be indicating a delayed start of the decrease in the aerosol loadings in the western part of the Alps, however we could not assess this hypothesis in this study. These results for these periods at high elevations, let us conclude that indirect aerosol effect might have played an important role in the all-sky SSR trends, together with direct aerosol effects and a minor contribution from changes in cloud cover (especially in the 1994-2006 period). However, the 1996-2020 period at high elevations in Austria shows statistically significant negative trends in clear-sky and true overcast SSR, despite the weak, but existing, decrease in AOD in Austria after 2000, shown in figure 5. In Switzerland the 2009-2020 period also shows negative trends in clear-sky SSR. As the physical processes discussed so far seem not to be sufficient to explain the clear-sky, true overcast and consequently all-sky SSR trends at the beginning of the 21st century, we analysed additional potential causes for the trends, namely water vapour and surface albedo.

3.4 Surface albedo and water vapour changes

Surface albedo has a strong effect on the diffuse component of the global radiation measured at the surface. In most tropical and subtropical areas, however, albedo changes are minor and associated primarily with land use change. Nonetheless, at high elevations in the Alps, the presence of snow and ice increase dramatically the surface albedo long term mean and seasonality. Thus, the potential effect of surface albedo on SSR interannual variability and decadal trends is expected to be higher at high elevations when compared to low elevations in the Alps. This is especially relevant in the context of global warming. Higher temperatures might lead to more snow and ice melting, thereby decreasing the surface albedo. Figure 7 displays the annual mean surface albedo decadal trend for the 1996-2020 period from ERA5 in the Alpine region.

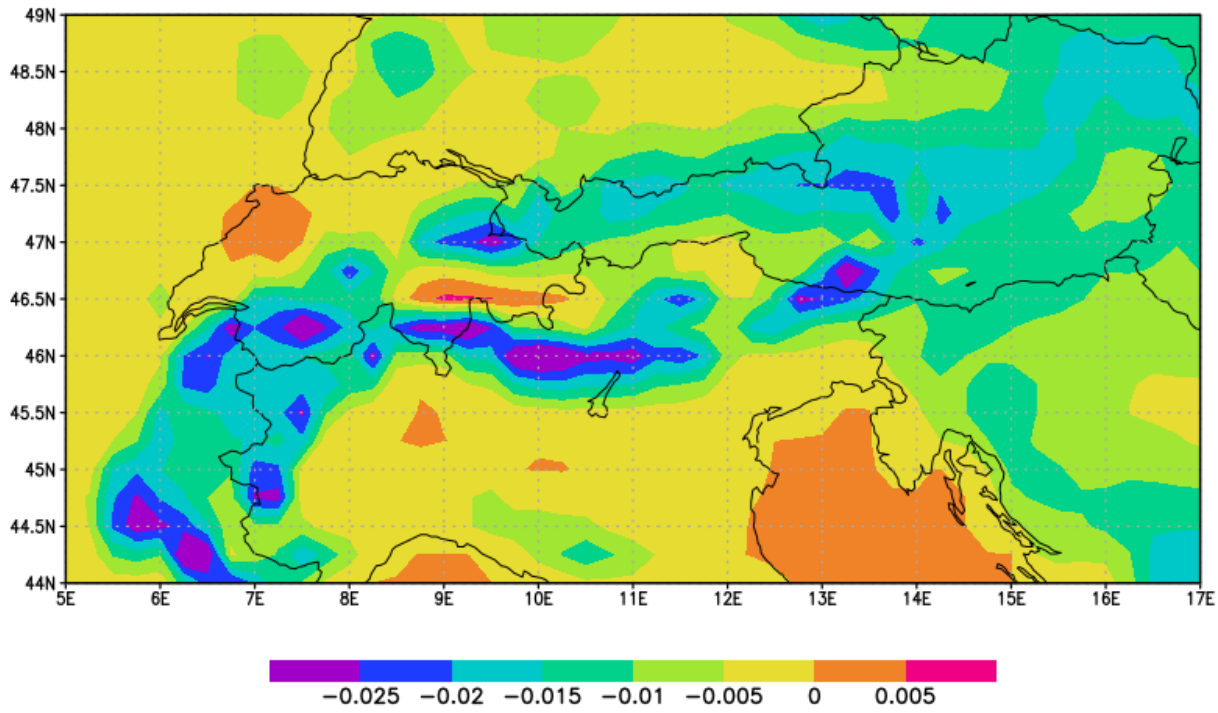

Figure 7 - Annual mean surface albedo trend (in decade^{-1}) from ERA5 for the 1996-2020 period.

The figure shows an overall negative trend in surface albedo in a region that follows the topography of the Alpine mountains, indicating a significative reduction in surface albedo at high elevations. The trends are mostly in a range between -1% and -2% per decade, even exceeding -2% per decade in some areas, and are statistically significant (not shown). As the all-sky SSR averaged over the high elevation stations as defined in table 1 is 154 W/m^2 and 145 W/m^2 in Switzerland and Austria respectively, this would mean a reduction between 1.4 and 3.1 W/m^2 per decade in the shortwave radiation reflected by the surface. This reduction in shortwave reflected radiation does not result directly in a reduction in SSR, as some of this radiation will just be lost to space, some absorbed in the atmosphere and only a fraction of it will be scattered back to the surface. On the other hand, the complex topography of the alps could also enhance the surface albedo effects, once the radiation reflection from other mountains or even from valleys could also contribute to the diffuse component of the global radiation, thus affecting SSR. In any case, the values estimated for the reduction in reflected SSR (not considering any of the above mentioned additional factors) suggest that this still might be a non negligible contribution to the observed SSR trends. In fact, the period of negative trends in surface albedo is a period of statistically significant dimming in Austria only at high elevations. This dimming is also observed in the clear-sky and the true overcast SSR, both scenarios where surface albedo effects

are not screened out during the derivation of the time series (clear-sky screens out cloud effects and true overcast screens out cloud-free processes).

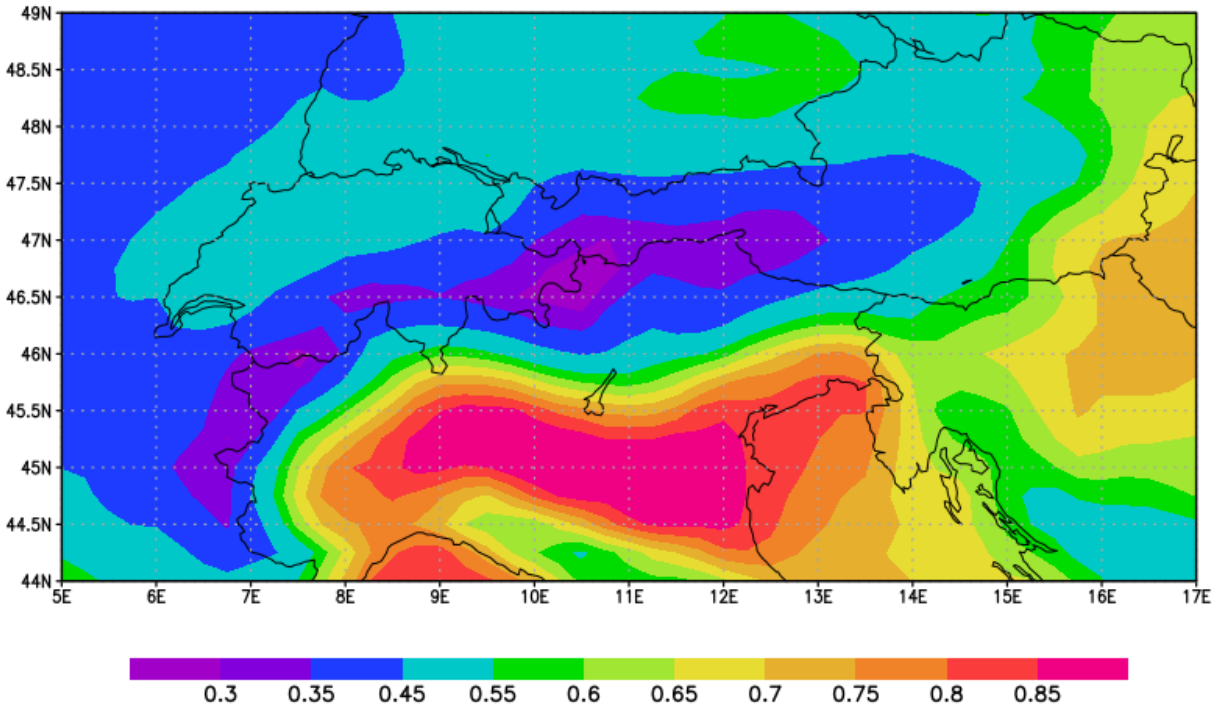

Figure 8 - Annual mean water vapour trend (in mm per decade) from ERA5 for the 1996-2020 period.

Figure 8 shows the annual mean water vapour trend for the 1996-2020 period in the region. The whole area shows positive trends in water vapour content in the atmosphere. Water vapor absorbs shortwave radiation, but its impacts are much lower than those of aerosol and clouds. Hakuba et al. (2016) derived an empirical equation to calculate atmospheric absorption at pristine locations based on the surface albedo and water vapour. Assuming the high elevation stations as pristine, and using that equation to calculate the change in atmospheric absorption that a positive trend of 0.3 mm per decade (trends over the Alps in figure 8) in water vapour would have in a location with average surface albedo of 0.3 (typical value for the annual means and 0.25 degree spatial resolution at high elevations in the Alps) and average SSR of 145 W/m^2, we find that this could increase atmospheric absorption of shortwave radiation by 0.8 W/m^2 per decade. More atmospheric absorption would lead to a corresponding decrease in SSR. This value is, however, of lower magnitude than the observed dimming in Austria in the 1996-2020 period. So the results show a potential contribution of an increase in water vapour to the observed dimming at high elevations in Austria in the period, but this contribution is rather minor, compared to other variables. Considering also that cloud cover at high elevations in Austria had a

near zero negative trend in the period and that the observed reduction in AOD cannot explain the observed dimming, these results suggest that a reduction in surface albedo played a significant role to the dimming observed at high elevations in Austria in the 1996-2020 period.

In the Swiss composites we observe a weaker brightening in the 2009-2020 period at high elevations when compared to low elevations. The same discussion of the surface albedo and water vapour contributions for the Austrian high elevation stations can be applied to the Swiss high elevation stations. We see, in fact, near zero/slightly negative trends in clear-sky SSR at the high altitudes in Switzerland in the period despite the negative trends in AOD. As previously highlighted, clear-sky SSR does not screen out the effects of both water vapour and surface albedo. Cloud cover also shows negative trends (albeit with large uncertainties) for the Swiss highlands in the period. This indicates a positive forcing to the SSR by changes in cloud cover (in addition to positive forcing by the AOD reduction due to direct and potentially also indirect aerosol effects), while negative forcing by surface albedo and water vapour, resulting in weaker brightening at high elevations when compared to low elevations. In contrast, at low elevations, reduction of aerosol loadings (which is already higher at low elevations) and a potential reduction in cloud cover (statistically insignificant) both provide positive forcing to SSR, resulting in a stronger brightening in the all-sky SSR.

4 Discussion

The results presented here strongly suggest that high elevation and low elevation Alpine stations are affected by different processes controlling the SSR decadal trends. At low altitude stations, clear-sky and all-sky SSR decadal trends were almost always consistent with each other. In addition to mostly weak and highly uncertain cloud cover trends, this indicates that the reduction in aerosol loadings, reported by Stern (2006) and presented in our results, played a major role in the decadal trends in SSR at low elevations of the Alpine region. This is in line with previous studies (e.g. Wild et al, 2005; Streets et al., 2009; Manara et al., 2016, Wild et al., 2021). Our results also indicated that this change in aerosol loadings may have not been homogeneous between western and eastern Alps. This is a potential reason for the observed earlier start and end of the brightening period in Austria: brightening already occurred in the 1980s and slowed down at the turn to the 21st century, while the Swiss stations only showed brightening since the 1990s, which continued until the end of the period of this study. This is indicated by the strong brightening in the Swiss low elevation composite observed during the 2009-2020 period, and reinforced by the strong brightening seen in Payerne in the 1996-2020 period, with Payerne being the only Swiss station where the trend in this period could be calculated.

On the other hand, at high elevations, a more complex combination of physical processes is behind the causes for the observed SSR trends. First, due to the lower aerosol concentrations at high elevations, the direct aerosol effect is less impactful. But this also means that indirect aerosol effects have a higher potential of causing SSR changes. The conceptual framework on the role of aerosols and clouds in Global Dimming and Brightening (Wild, 2009, 2012) suggests that at pristine locations the indirect aerosol effect can be of significant importance for the SSR trends, strongly affecting cloud optical depth and cloud lifetime. Such pristine conditions can be

found at the high elevation sites analysed in this study. Second, the more frequent presence of snow and ice at high elevations makes the surface albedo a more relevant aspect at these stations. Especially in the context of global warming, once higher temperatures can melt more snow and ice, this reduces the surface albedo and thereby SSR through reduced multiple scattering between the surface and the overlying atmosphere.

At high elevations cloud cover trends were, in most cases, either near zero or highly uncertain, indicating that they did not play a dominant role to the observed SSR trends. In such a complex scenario, with no obvious strong cloud cover contribution to the trends, a combination of the other relevant factors must have contributed to the observed SSR trends. Statistically significant trends under true overcast conditions at high elevations indicated that changes in cloud optical properties, potentially resulting from aerosol indirect effect, are in fact more relevant at high elevations than at low elevations. This fits to the theory and also to observations from Juranyi et al. (2011) which have shown that cloud droplet activation is likely to occur most of the time in aerosol limited regimes at Jungfraujoch. Based on such results, one might conclude that changes in aerosol loadings (more or less CCNs) would be reflected more in aerosol indirect effects than in aerosol direct effects or in cloud cover changes at pristine high elevation sites. Our results show significant contributions of true overcast conditions to the SSR trends, and consequently cloud optical properties, mostly in the 1994-2006 period both in Switzerland and in Austria. But this significant contribution can also be extended to the 1981-1994 period in Switzerland and to the 1996-2020 period for Austria. For the time windows between 1981 and 2006, the true overcast SSR trends fit to the previously documented and observed changes in AOD. The same cannot be said about the 1996-2020 period in Austria, meaning that additional investigations on the cloud optical properties or other potentially relevant contributors to the SSR decadal trends would be needed. Cloud optical properties can be affected by indirect aerosol effects but also by other aspects not assessed in this study, such as cloud liquid water content. Thus, even though the results and the literature (e.g. Krüger and Graßl, 2002) point towards changes in cloud optical depth due to changes in aerosol loadings, we could not further challenge the hypothesis that the changes in cloud optical depth were in fact due to indirect aerosol effect. In all these periods, a minor contribution from the direct aerosol effect should also be taken into consideration at high elevations.

At the end of the 20th century and beginning of the 21st century, changes in surface albedo may also have contributed to the SSR trends at high elevation Alpine stations. The 1996-2020 period at the Austrian stations is especially remarkable in this regard. A statistically significant dimming is observed only at high elevations over this period, while low elevation stations show near zero trends. Cloud cover trends are near zero in both low and high elevations, and clear-sky and true overcast SSR show statistically significant negative trends only at high elevations. If such all-sky SSR negative trends at high elevations would be mostly associated with changes in aerosol loadings, an expected outcome would also be negative trends in clear-sky SSR at low elevations, which was not observed. Furthermore, our results also show small reductions in AOD in the beginning of the 21st century. So it is unlikely that some aerosol changes dominate these SSR trends. This period showed, however, strong negative trends in surface albedo at high elevations (>0.015 per decade). As the influence of surface albedo is not

screened out neither in the clear-sky nor the true overcast SSR time series, any potential effect of this variable would be present in both derived time series. Thus, our results suggest a strong contribution of surface albedo reduction to the dimming observed in the high elevation Austrian stations in the 1996-2020 period, with some minor contribution of water vapour content increase, as presented in the results section.

At the Swiss high elevation stations, the 2009-2020 period showed statistically insignificant positive trends in all-sky SSR, in contrast to statistically significant trends at low elevations. From the AOD trends map we see that the aerosol reduction at the beginning of the 21st century was stronger in Switzerland than in Austria. This, together with negative (but highly uncertain) cloud cover trends, is very likely the reason why the Swiss stations show continued brightening. The same surface albedo effect as at the high elevation Austrian stations is, however, also expected to be present at high elevation Swiss stations. As a reduction in surface albedo exerts a negative forcing onto SSR, this could be one of the main reasons for the lower all-sky SSR trends at the Swiss high elevations when compared to low elevations. Table 3 summarises our results, indicating the main contributions for every time window analysed in this study.

	1981-1994	1994-2006	2009-2020	1996-2020
Swiss low elevation	AOD with minor contribution from CC	AOD with minor contribution from CC	AOD with minor contribution from CC	-
Swiss high elevation	COP	COP with minor contribution from CC and from AOD	Positive forcing by CC, AOD and COP; negative forcing by WV and SA	-
Austrian low elevation	AOD	AOD	-	Near zero trends
Austrian high elevation	AOD and CC	COP	-	SA with minor contribution from WV

Table 3 - Summary of the most important drivers of the all-sky SSR trends for each composite in each time window. The 2009-2020 period in Austria is not included to rather focus on the longer 1996-2020 period, which is available for Austrian composites. Dark red indicates statistically significant brightening; light red indicates statistically insignificant brightening; dark blue indicates statistically significant dimming; light blue indicates statistically insignificant dimming; and white indicates statistically insignificant trend between -1 and 1 W/m² per decade. CC = Cloud cover; COP = Cloud optical properties (possibly associated with indirect aerosol effect); AOD = Aerosol Optical Depth, refers to direct aerosol effect; WV = water vapour; and SA = Surface Albedo.

Even though here we highlighted the effects of changes in cloud optical depth and surface albedo on the SSR trends, the changes in cloud cover should also be considered, particularly when discussing inter-annual variations. All four composites show a very positive all-sky SSR anomaly in the year 2003, for example, which has been reported as an anomalous dry and hot year in Central Europe (Garcia-Herrera et al., 2010). It is likely that trends in cloud cover would

dominate over any trends in cloud optical depth, thus, we emphasise that the observed trends at high altitudes occurred mostly without major cloud cover trends.

5 Conclusions

In this study we investigated the decadal SSR trends at low and high elevations in the Swiss and Austrian Alps, and discussed their causes. The analysis of four composite time series revealed spatio-temporal differences in the SSR trends in the region: At the Western (Swiss) stations, both at high low and high altitudes, SSR brightening started in the early 1990s and continued after 2000, while the Eastern (Austrian) stations showed a brightening phase already occurring in the 1980s and slowing down after 2000. This contrast is also evident in the AOD trends after 2000, with stronger negative trends in AOD in Switzerland than in Austria. Further comparison between low elevation and high elevation sites revealed that at lower altitudes the decadal SSR trends were mostly determined by clear-sky processes, most likely related to the changes in aerosol loadings starting to decline in the last decades of the 20th century in Europe. At high altitude sites, on the other hand, clear-sky trends accounted for a smaller portion of the total all-sky long term variability. After the identification of no major decadal changes in cloud cover in most of the periods/composites, further analysis suggested that different processes contributed to the decadal SSR trends at high elevations. Minor contributions of water vapour and direct aerosol effects could be identified at the high elevation stations. Major contributions of changes in cloud optical depth mostly before and up to the 1994-2006 period and from changes in surface albedo for the 1996-2020 period in Austria and the 2009-2020 period in Switzerland could also be identified. The contributions from cloud optical properties could be associated with the aerosol indirect effect, as we can expect from the reduction of aerosol concentrations in the Alpine region and from the related conceptual framework on the role of aerosols and clouds in the Global Dimming and Brightening phenomenon under pristine and polluted conditions (Wild, 2009). But since we did not assess all aspects that could affect the cloud optical depth, additional analyses could still be performed to further test the hypothesis that the changes in cloud optical properties were associated mostly with aerosol indirect effect in the pristine high elevations. Nevertheless, the results lead us to conclude that changes in cloud optical depth and in surface albedo have had a major impact on the decadal trends of SSR at high altitudes in the Alps in the period of study. We highlight that the periods with identified contributions from cloud optical properties and surface albedo had mostly near zero or highly uncertain cloud cover trends. And we understand that changes in cloud cover could outweigh the impacts of cloud optical depth or surface albedo on the SSR trends. Thus, in the future these latter variables could still contribute significantly to the SSR decadal trends as long as there are no major changes in cloud cover. The hypothesis that the changes in cloud optical depth in the Alps were caused mostly by the indirect aerosol effect should, however, still be subject of further research.

Acknowledgments

This study was funded by the Swiss National Science Foundation grant no. 200020_188601.
Global dimming and brightening research at ETH is supported by the Federal Office of Meteorology and Climatology MeteoSwiss within the framework of GCOS Switzerland. through

their co-funding of the Global Energy Balance Archive (GEBA). We acknowledge the anonymous reviewers for their very constructive comments.

Data Availability Statement

The BSRN SSR data is available at the BSRN website (https://bsrn.awi.de/data/data-retrieval-via-ftp/). For this study it was retrieved via the ftp server ftp://ftp.bsrn.awi.de/. The WRDC SSR data is available for registered users at http://wrdc.mgo.rssi.ru/. The MeteoSwiss/ IDAWEB SSR, cloud cover and sunshine duration data is available for registered users at (https://gate.meteoswiss.ch/idaweb). Synop cloud cover, and sunshine duration data from the European Climate Assessment & Dataset website can be downloaded at (https://www.ecad.eu/dailydata/index.php). The CAMS AOD reanalysis data is available under https://ads.atmosphere.copernicus.eu/cdsapp#!/dataset/cams-global-reanalysis-eac4-monthly?tab=form . The GeoSphere Austria SSR, cloud cover and sunshine duration data is available at https://data.hub.geosphere.at/group/stationsdaten .

References

Beguería, S., Tomas-Burguera, M., Serrano-Notivoli, R., Peña-Angulo, D., Vicente-Serrano, S. M., & González-Hidalgo, J. C. (2019). Gap filling of monthly temperature data and its effect on climatic variability and trends. *Journal of Climate*, *32*(22), 7797-7821.

Chtirkova, B., Folini, D., Correa, L. F., & Wild, M. (2022). Internal Variability of All-Sky and Clear-Sky Surface Solar Radiation on Decadal Timescales. *Journal of Geophysical Research: Atmospheres*, *127*(12), e2021JD036332.

Correa, L. F., Folini, D., Chtirkova, B., & Wild, M. (2022). A method for clear-sky identification and long-term trends assessment using daily surface solar radiation records. *Earth and Space Science*, e2021EA002197.

Driemel, A., Augustine, J., Behrens, K., Colle, S., Cox, C., Cuevas-Agulló, E., ... König-Langlo, G. (2018). Baseline Surface Radiation Network (BSRN): structure and data description (1992–2017) [Dataset]. *Earth System Science Data*, *10*(3), 1491-1501. doi:10.5194/essd-10-1491-2018

Dutton, E. G., Stone, R. S., Nelson, D. W., & Mendonca, B. G. (1991). Recent interannual variations in solar radiation, cloudiness, and surface temperature at the South Pole. *Journal of Climate*, *4*(8), 848-858.

Folini, D., Dallafior, T. N., Hakuba, M. Z., & Wild, M. (2017). Trends of surface solar radiation in unforced CMIP5 simulations. *Journal of Geophysical Research: Atmospheres*, *122*(1), 469-484.

García-Herrera, R., Díaz, J., Trigo, R. M., Luterbacher, J., & Fischer, E. M. (2010). A review of the European summer heat wave of 2003. *Critical Reviews in Environmental Science and Technology*, *40*(4), 267-306.

GeoSphere Austria Data Hub (2023) [Dataset]. Available online: https://data.hub.geosphere.at/group/stationsdaten

Gilgen, H., Wild, M., & Ohmura, A. (1998). Means and trends of shortwave irradiance at the surface estimated from global energy balance archive data. *Journal of Climate*, *11*(8), 2042-2061.

Hakuba, M. Z., Folini, D., & Wild, M. (2016). On the zonal near-constancy of fractional solar absorption in the atmosphere. *Journal of Climate*, *29*(9), 3423-3440.

Hersbach, H., Bell, B., Berrisford, P., Hirahara, S., Horányi, A., Muñoz-Sabater, J., ... & Thépaut, J. N. (2020). The ERA5 global reanalysis. *Quarterly Journal of the Royal Meteorological Society*, *146*(730), 1999-2049.

Hogan, R. (2015). Radiation Quantities in the ECMWF model and MARS. *ECMWF, 2016.*

IDAWEB repository, Meteoswiss (2023) [Dataset]. Available online: https://gate.meteoswiss.ch/idaweb

Inness, A., Ades, M., Agustí-Panareda, A., Barré, J., Benedictow, A., Blechschmidt, A. M., ... & Suttie, M. (2019). The CAMS reanalysis of atmospheric composition [Dataset]. *Atmospheric Chemistry and Physics*, *19*(6), 3515-3556. https://doi.org/10.5194/acp-19-3515-2019

Jurányi, Z., Gysel, M., Weingartner, E., Bukowiecki, N., Kammermann, L., & Baltensperger, U. (2011). A 17 month climatology of the cloud condensation nuclei number concentration at the high alpine site Jungfraujoch. *Journal of Geophysical Research: Atmospheres*, *116*(D10).

Kendall, M. G. (1975). Rank correlation methods. 2nd impression. *Charles Griffin and Company Ltd. London and High Wycombe*.

Klein Tank, A. M. G., Wijngaard, J. B., Können, G. P., Böhm, R., Demarée, G., Gocheva, A., ... & Petrovic, P. (2002). Daily dataset of 20th-century surface air temperature and precipitation series for the European Climate Assessment [Dataset]. *International Journal of Climatology: A Journal of the Royal Meteorological Society*, *22*(12), 1441-1453. https://doi.org/10.1002/joc.773

Krüger, O., & Graßl, H. (2002). The indirect aerosol effect over Europe. *Geophysical Research Letters*, *29*(19), 31-1.

Long, C. N., & Dutton, E. G. (2002). BSRN Global Network Recommended QC Tests,V 2.0: BSRN Technical Report.

Manara, V., Brunetti, M., Celozzi, A., Maugeri, M., Sanchez-Lorenzo, A., & Wild, M. (2016). Detection of dimming/brightening in Italy from homogenized all-sky and clear-sky

surface solar radiation records and underlying causes (1959–2013). *Atmospheric Chemistry and Physics*, *16*(17), 11145-11161.

Mann, H. B. (1945). Nonparametric tests against trend. *Econometrica: Journal of the econometric society*, 245-259.

Nishizawa, S., & Yoden, S. (2005). Distribution functions of a spurious trend in a finite length data set with natural variability: Statistical considerations and a numerical experiment with a global circulation model. *Journal of Geophysical Research: Atmospheres*, *110*(D12).

Norris, J. R., & Wild, M. (2007). Trends in aerosol radiative effects over Europe inferred from observed cloud cover, solar "dimming," and solar "brightening". *Journal of Geophysical Research: Atmospheres*, *112*(D8).

Ohmura, A., & Lang, H. (1989). Secular variation of global radiation over Europe, in Current Problems in Atmospheric Radiation. *edited by J. Lenoble, & JF Geleyn*, *98*, 301.

Ohmura, A., Dutton, E. G., Forgan, B., Fröhlich, C., Gilgen, H., Hegner, H., ... Wild, M. (1998). Baseline Surface Radiation Network (BSRN/WCRP): New precision radiometry for climate research. *Bulletin of the American Meteorological Society*, *79*(10), 2115-2136.

Philipona, R. (2013). Greenhouse warming and solar brightening in and around the Alps. *International journal of climatology*, *33*(6), 1530-1537.

Power, H. C. (2003). Trends in solar radiation over Germany and an assessment of the role of aerosols and sunshine duration. *Theoretical and Applied Climatology*, *76*(1), 47-63.

Rotach, M. W., & Zardi, D. (2007). On the boundary-layer structure over highly complex terrain: Key findings from MAP. *Quarterly Journal of the Royal Meteorological Society: A journal of the atmospheric sciences, applied meteorology and physical oceanography*, *133*(625), 937-948.

Ruckstuhl, C., Philipona, R., Morland, J., & Ohmura, A. (2007). Observed relationship between surface specific humidity, integrated water vapor, and longwave downward radiation at different altitudes. *Journal of Geophysical Research: Atmospheres*, *112*(D3).

Ruckstuhl, C., Norris, J. R., & Philipona, R. (2010). Is there evidence for an aerosol indirect effect during the recent aerosol optical depth decline in Europe?. *Journal of Geophysical Research: Atmospheres*, *115*(D4).

Russak, V. (1990). Trends of solar radiation, cloudiness and atmospheric transparency during recent decades in Estonia. *Tellus B*, *42*(2), 206-210.

Sen, P. K. (1968). Estimates of the regression coefficient based on Kendall's tau. *Journal of the American statistical association*, *63*(324), 1379-1389.

Serafin, S., Adler, B., Cuxart, J., De Wekker, S. F., Gohm, A., Grisogono, B., ... & Zardi, D. (2018). Exchange processes in the atmospheric boundary layer over mountainous terrain. *Atmosphere*, *9*(3), 102.

Stanhill, G., & Moreshet, S. (1992). Global radiation climate changes: The world network. *Climatic Change*, *21*(1), 57-75

Stern, D. I. (2006). Reversal of the trend in global anthropogenic sulfur emissions. *Global Environmental Change*, *16*(2), 207-220.

Stjern, C. W., Kristjánsson, J. E., & Hansen, A. W. (2009). Global dimming and global brightening—An analysis of surface radiation and cloud cover data in northern Europe. *International Journal of Climatology: A Journal of the Royal Meteorological Society*, *29*(5), 643-653.

Streets, D. G., Yan, F., Chin, M., Diehl, T., Mahowald, N., Schultz, M., ... & Yu, C. (2009). Anthropogenic and natural contributions to regional trends in aerosol optical depth, 1980–2006. *Journal of Geophysical Research: Atmospheres*, *114*(D10).

Voeikov Main Geophysical Observatory. (2022) [Dataset]. World Radiation Data Centre website. http://wrdc.mgo.rssi.ru/

Wang, X. L. (2008). Penalized maximal F test for detecting undocumented mean shift without trend change. *Journal of Atmospheric and Oceanic Technology*, *25*(3), 368-384.

Weatherhead, E. C., Reinsel, G. C., Tiao, G. C., Meng, X. L., Choi, D., Cheang, W. K., ... & Frederick, J. E. (1998). Factors affecting the detection of trends: Statistical considerations and applications to environmental data. *Journal of Geophysical Research: Atmospheres*, *103*(D14), 17149-17161.

Wild, M., Gilgen, H., Roesch, A., Ohmura, A., Long, C. N., Dutton, E. G., ... & Tsvetkov, A. (2005). From dimming to brightening: Decadal changes in solar radiation at Earth's surface. *Science*, *308*(5723), 847-850.

Wild, M. (2009). Global dimming and brightening: A review. *Journal of Geophysical Research: Atmospheres*, *114*(D10).

Wild, M. (2012). Enlightening global dimming and brightening. *Bulletin of the American Meteorological Society*, *93*(1), 27-37.

Wild, M., Wacker, S., Yang, S., & Sanchez-Lorenzo, A. (2021). Evidence for clear-sky dimming and brightening in central Europe. *Geophysical Research Letters*, *48*(6), e2020GL092216.

Yang, S., Zhou, Z., Yu, Y., & Wild, M. (2021). Cloud ‘shrinking’and ‘optical thinning’in the ‘dimming’period and a subsequent recovery in the ‘brightening’period over China. *Environmental Research Letters*, *16*(3), 034013.

Figure 1.

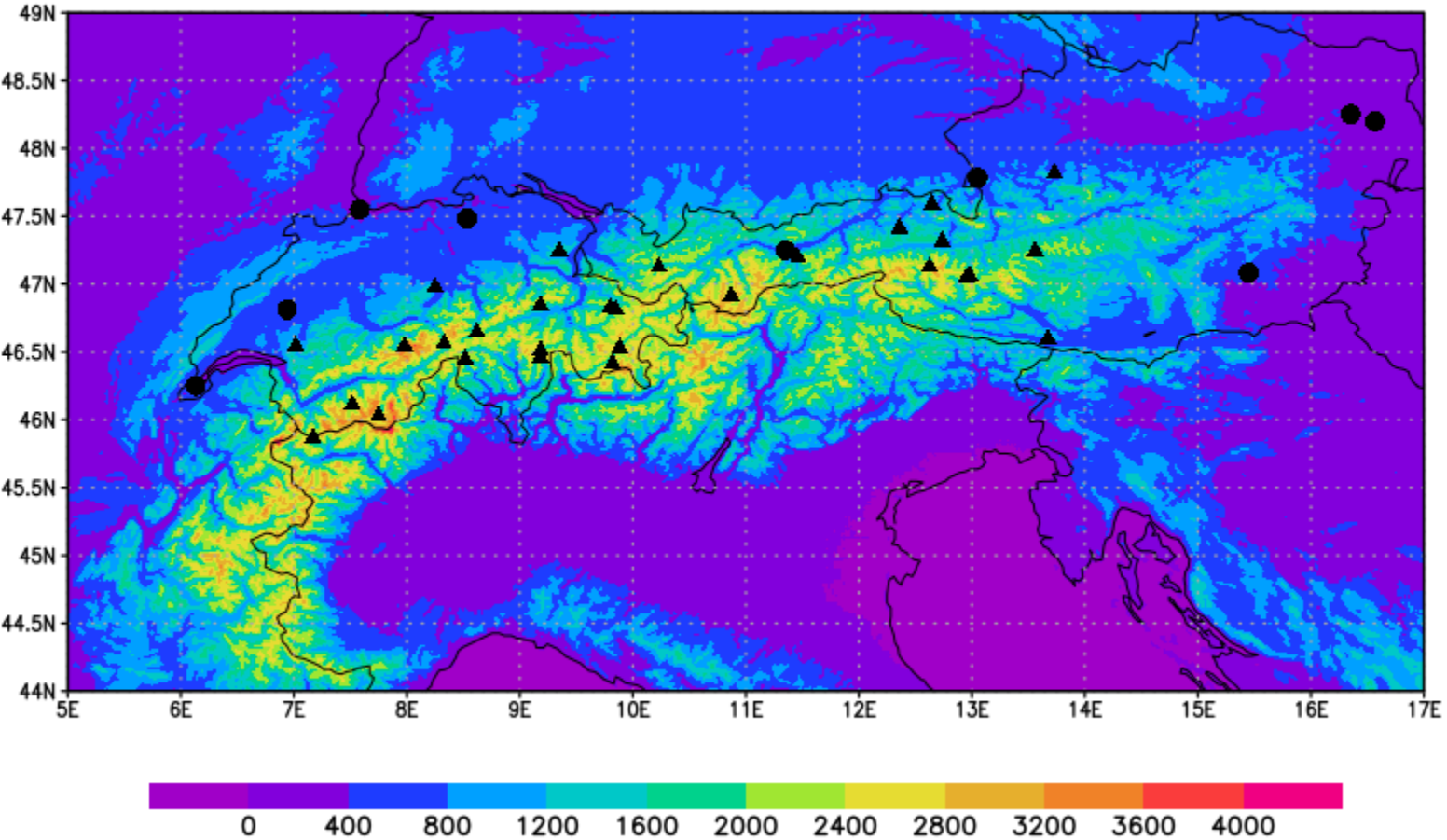
49N
48.5N
48N
47.5N
47N
46.5N
46N
45.5N
45N
44.5N
44N
5E
6E
7E
8E
9E
10E
11E
12E
13E
14E
15E
16E
17E
0
400
800
1200
1600
2000
2400
2800
3200
3600
4000

Figure 2.

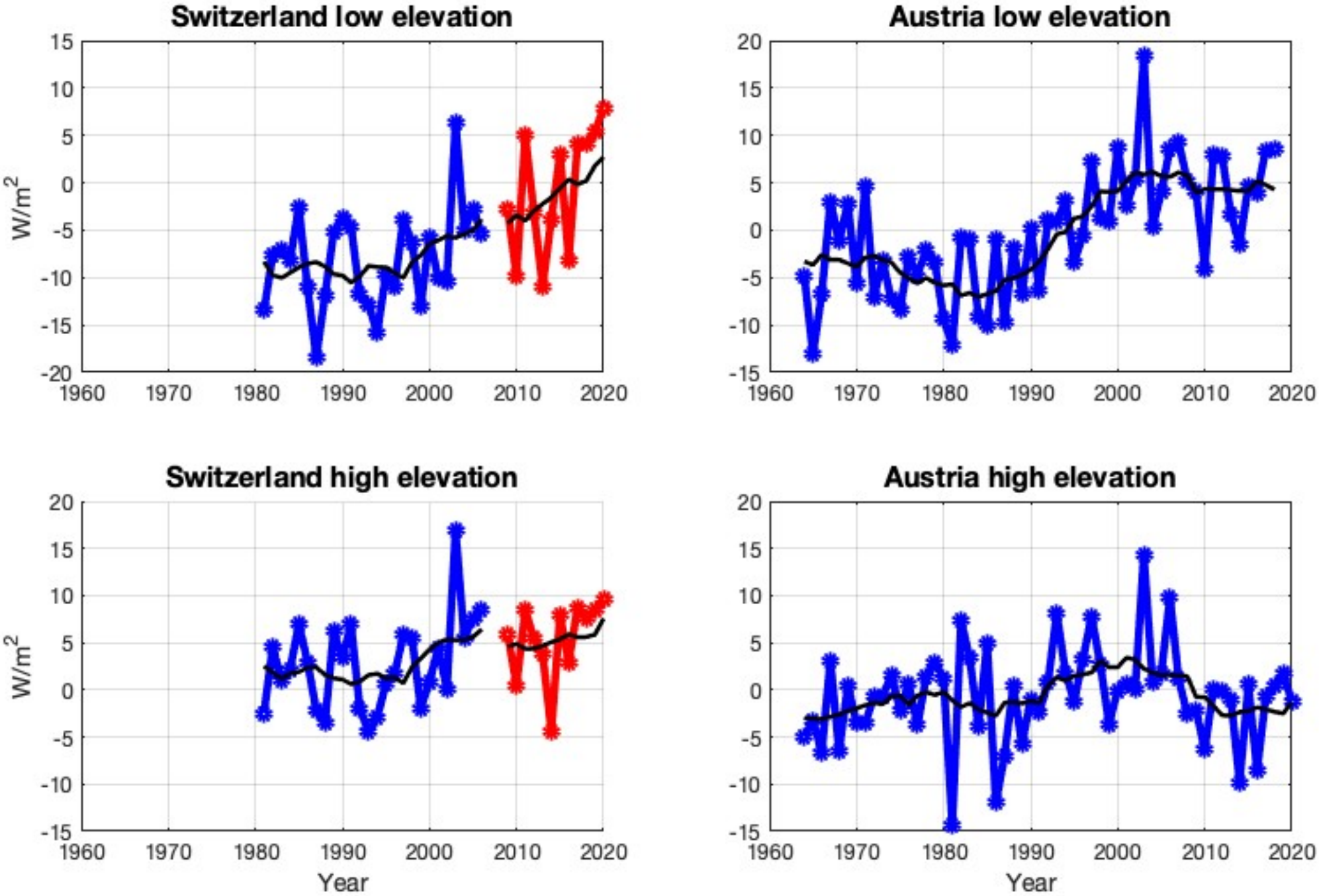
Switzerland low elevation
Austria low elevation
Switzerland high elevation
Austria high elevation
W/m2
Year
1960
1970
1980
1990
2000
2010
2020

Figure 3.

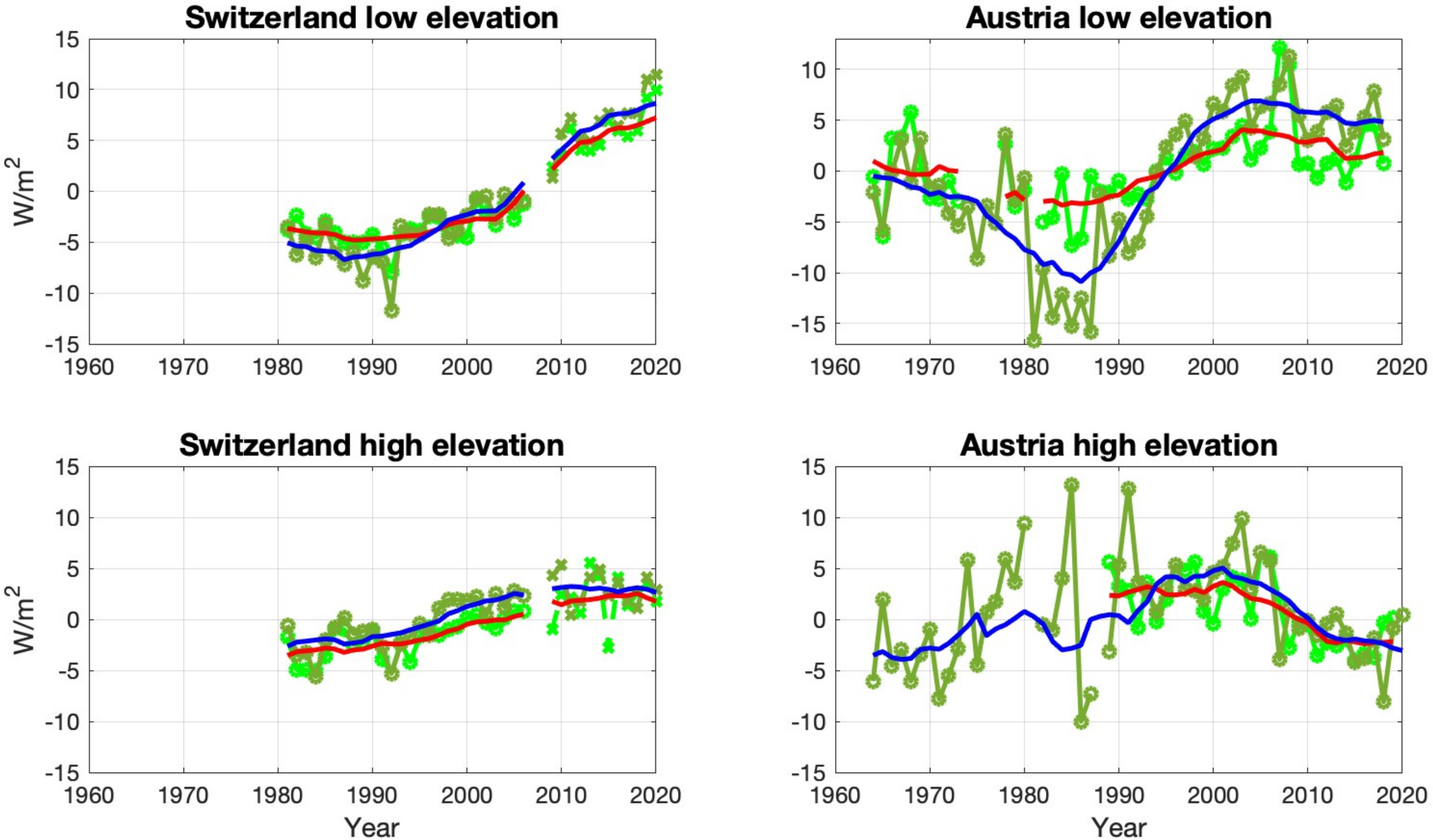
Switzerland low elevation
Austria low elevation
Switzerland high elevation
Austria high elevation
W/m2
Year
15
10
5
0
-5
-10
-15
1960
1970
1980
1990
2000
2010
2020

Figure 4.

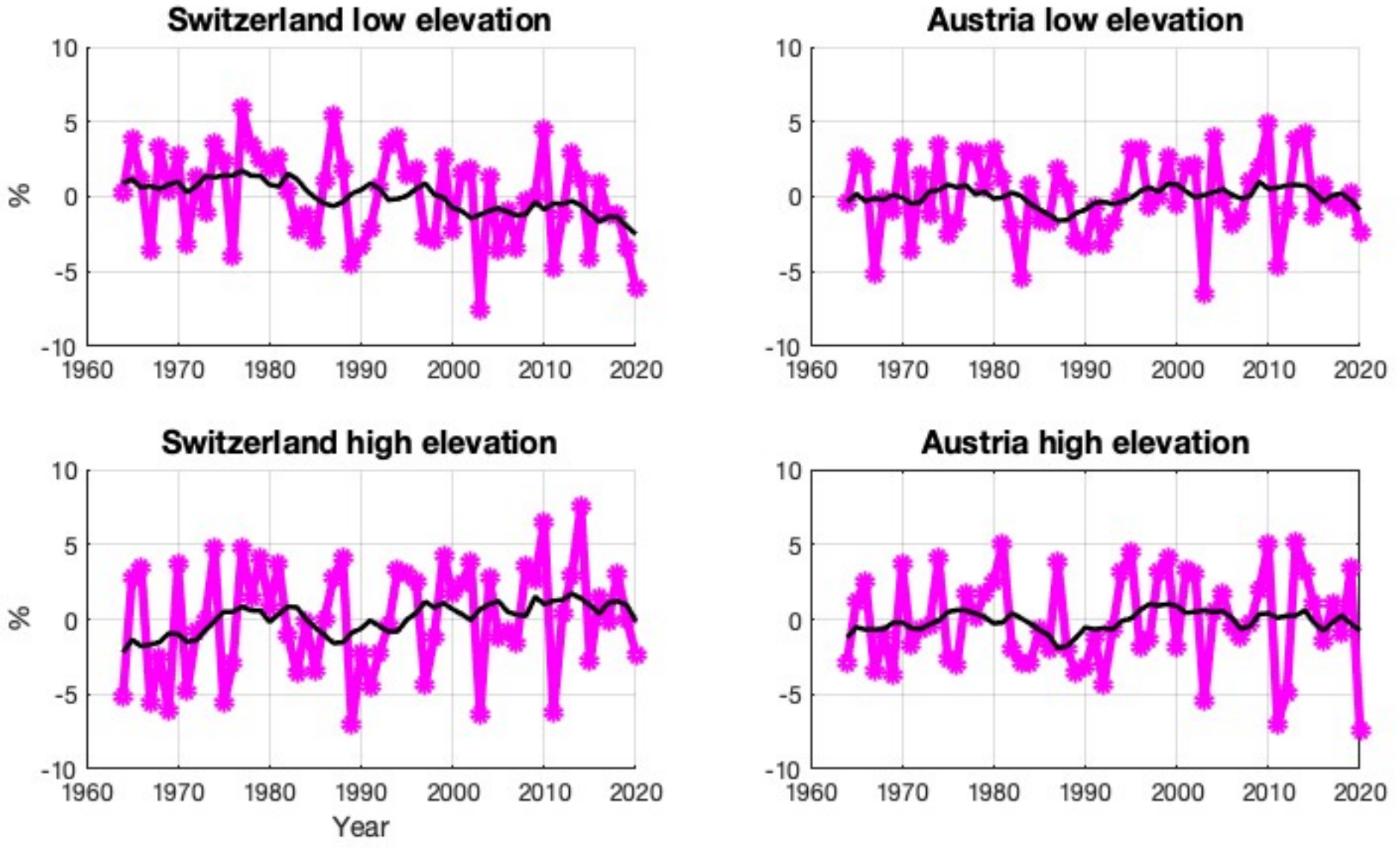
Switzerland low elevation
Austria low elevation
Switzerland high elevation
Austria high elevation
%
Year
10
5
0
-5
-10
1960
1970
1980
1990
2000
2010
2020

Figure 5.

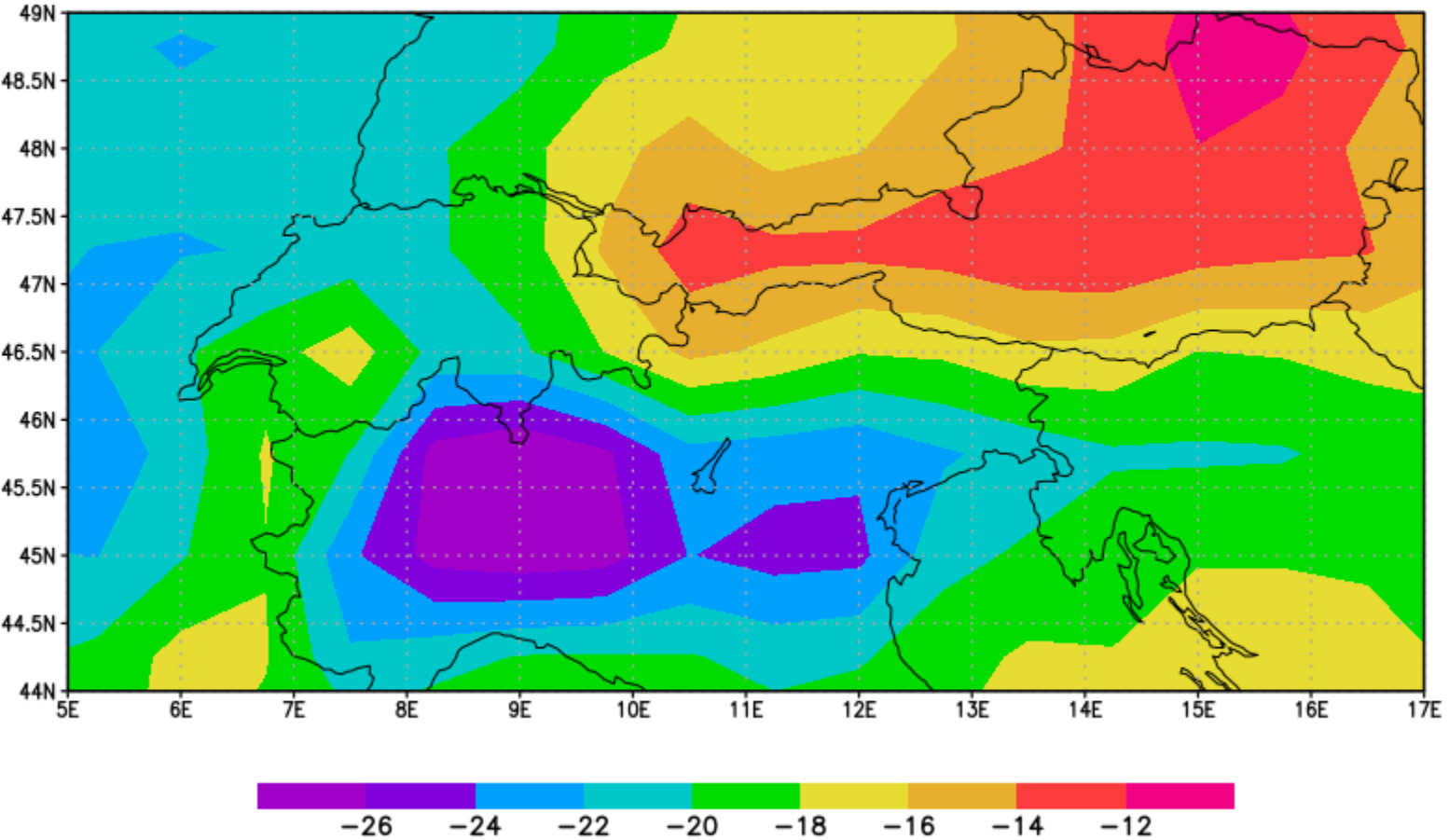
49N
48.5N
48N
47.5N
47N
46.5N
46N
45.5N
45N
44.5N
44N
5E
6E
7E
8E
9E
10E
11E
12E
13E
14E
15E
16E
17E
−26
−24
−22
−20
−18
−16
−14
−12

Figure 6.

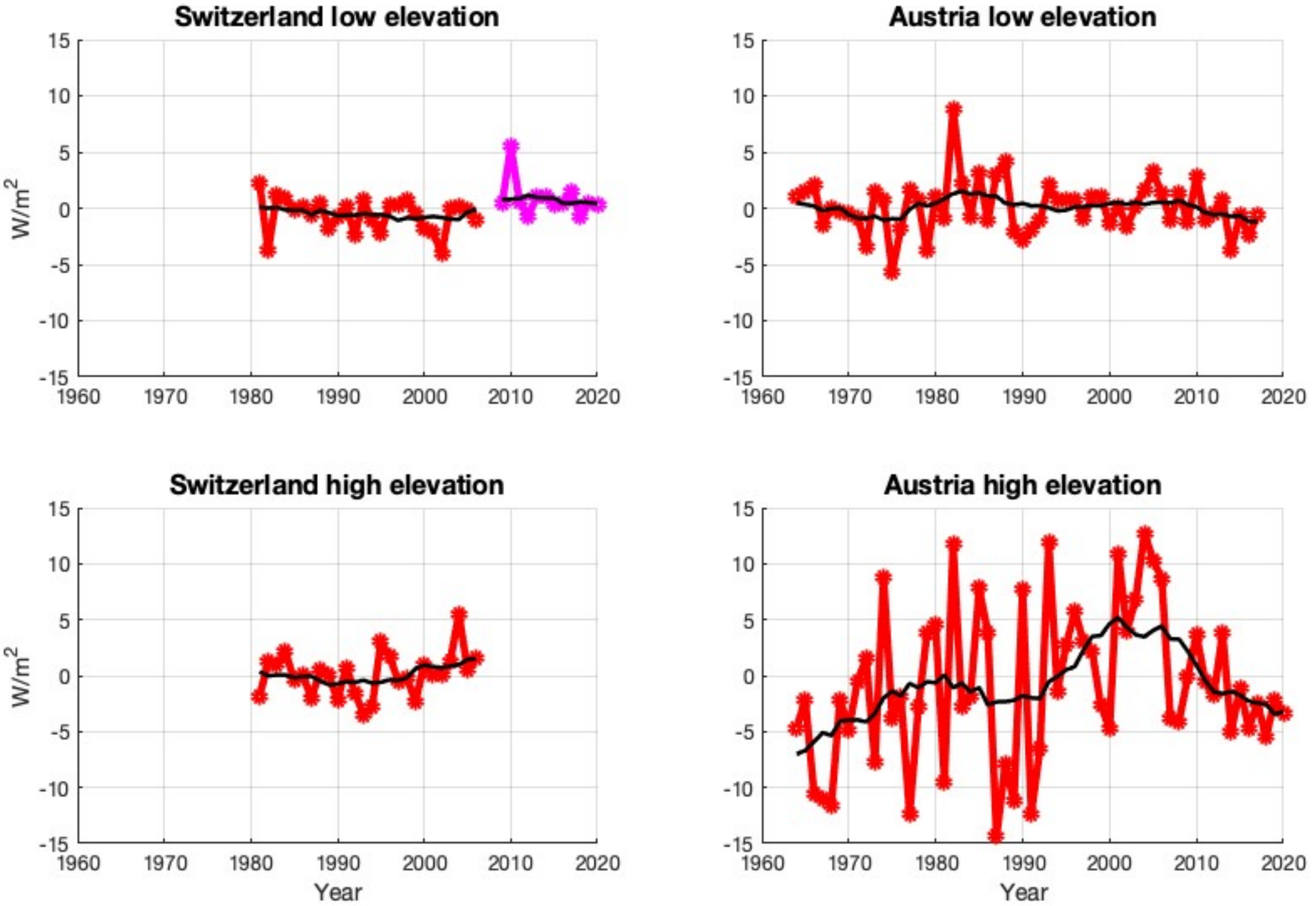
Switzerland low elevation
Austria low elevation
Switzerland high elevation
Austria high elevation
W/m2
Year
15
10
5
0
-5
-10
-15
1960
1970
1980
1990
2000
2010
2020

Figure 7.

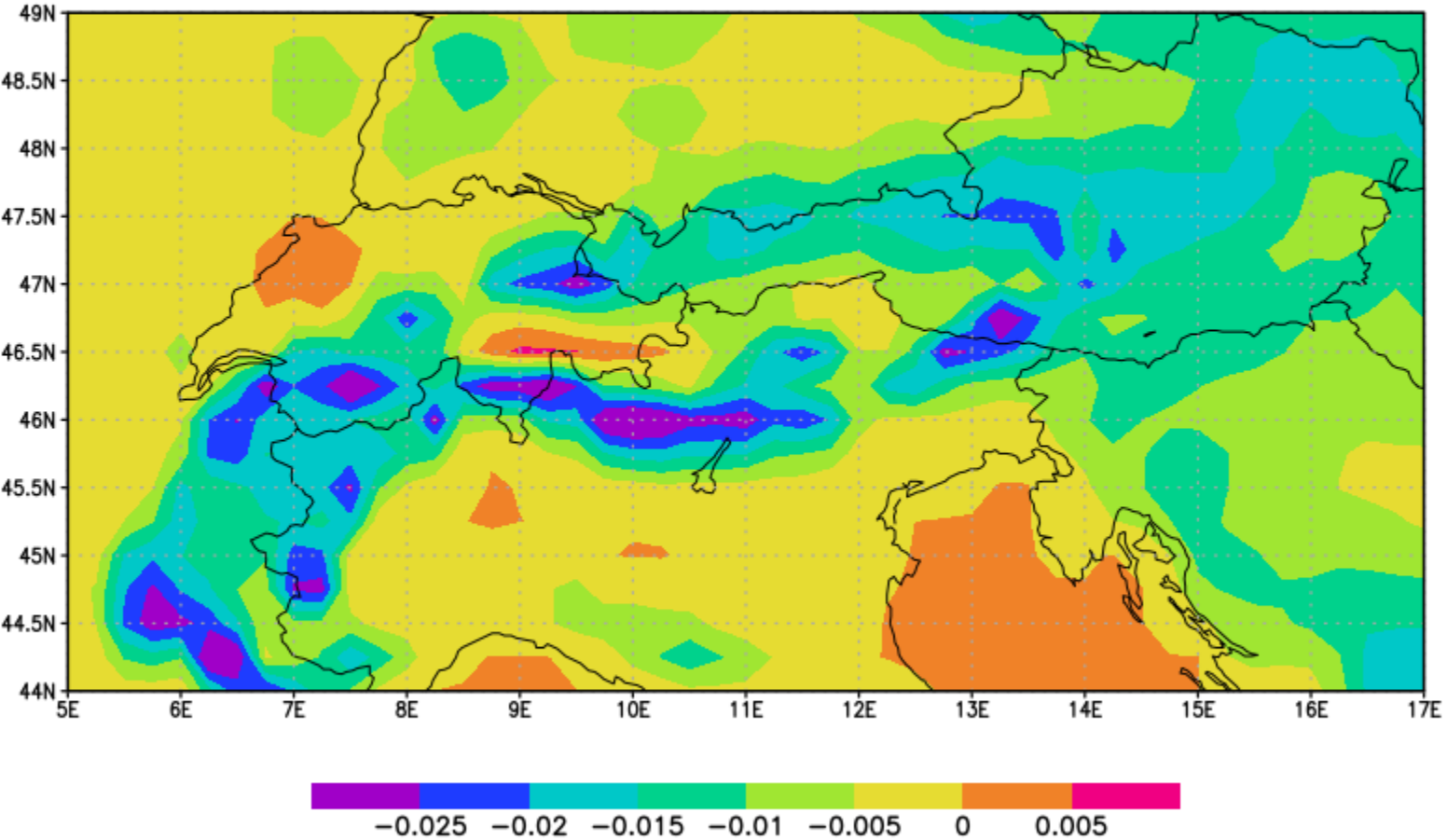
49N
48.5N
48N
47.5N
47N
46.5N
46N
45.5N
45N
44.5N
44N
5E
6E
7E
8E
9E
10E
11E
12E
13E
14E
15E
16E
17E
−0.025
−0.02
−0.015
−0.01
−0.005
0
0.005

Figure 8.

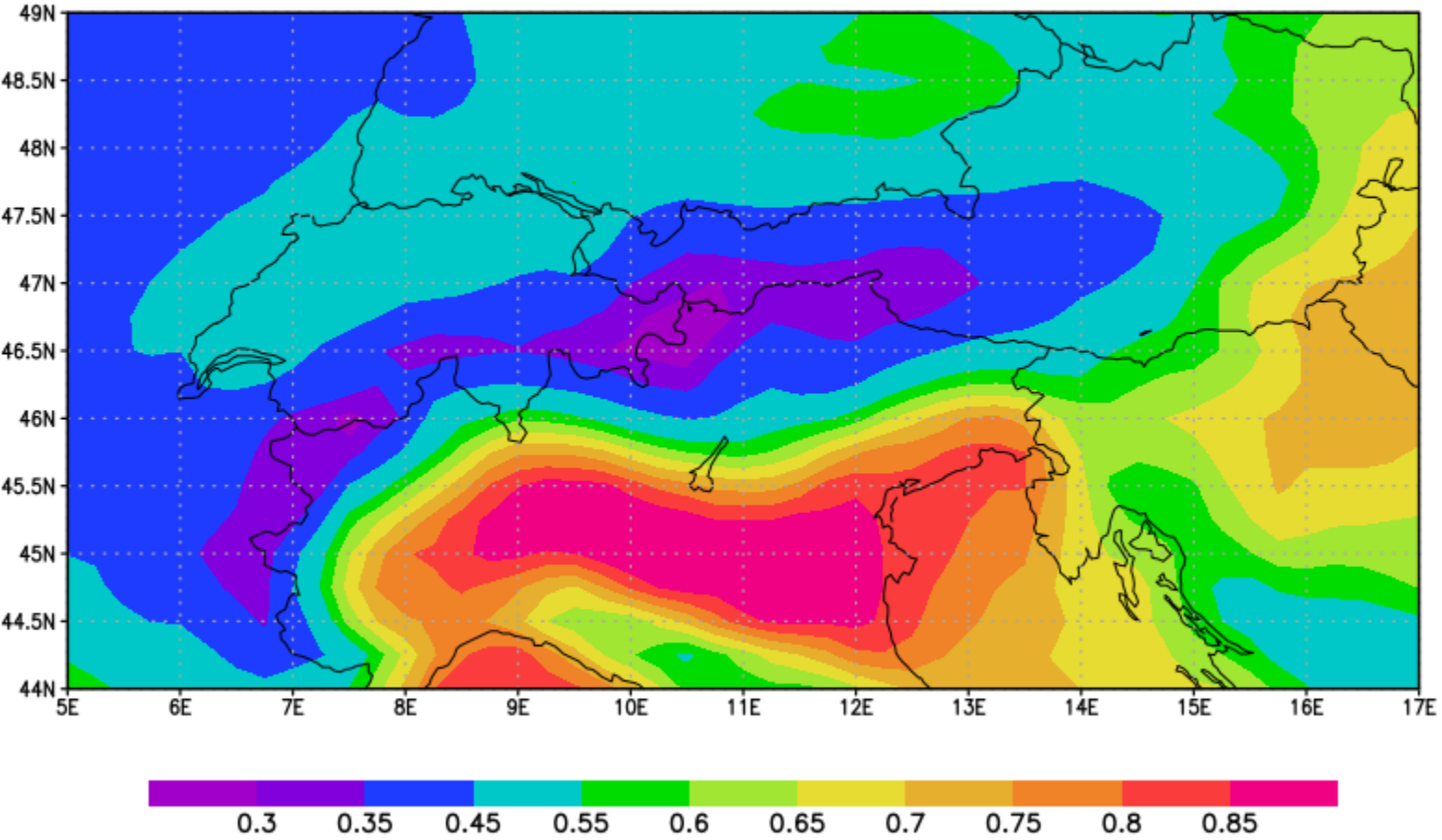
49N
48.5N
48N
47.5N
47N
46.5N
46N
45.5N
45N
44.5N
44N
5E
6E
7E
8E
9E
10E
11E
12E
13E
14E
15E
16E
17E
0.3
0.35
0.45
0.55
0.6
0.65
0.7
0.75
0.8
0.85